AD-A064 404 AIR FORCE INST OF TECH WRIGHT-PATTERSON AFB OHIO SCH--ETC F/G 20/6
COHERENCE PROPERTIES OF BROADBAND OPTICAL FIELDS WITH APPLICATI--ETC(U)
DEC 78 P S IDELL

UNCLASSIFIED AFIT/GEO/EE/78-1 NL

1 OF 2
AD
A064404

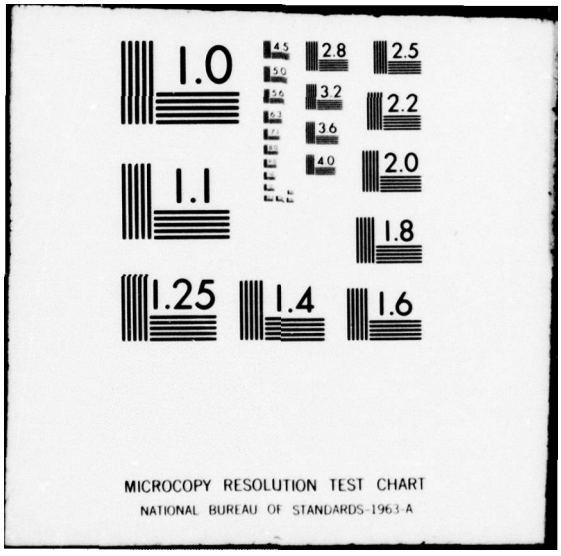
1.0
1.1
1.25
1.4
1.6
1.8
2.0
2.2
2.5
2.8
3.2
3.6
4.0
4.5
5.0
5.6
6.3
MICROCOPY RESOLUTION TEST CHART
NATIONAL BUREAU OF STANDARDS-1963-A

AD A064404

DDC FILE COPY

DDC

B.S.

LEVEL II

DDC
FEB 12 1979
A

UNITED STATES AIR FORCE
AIR UNIVERSITY
AIR FORCE INSTITUTE OF TECHNOLOGY
Wright-Patterson Air Force Base, Ohio

DISTRIBUTION STATEMENT A
Approved for public release;
Distribution Unlimited

79 01 30 146

AFIT/GEO/EE/78-1

LEVEL II

1

DDC FILE COPY AD A064404

COHERENCE PROPERTIES OF BROADBAND OPTICAL FIELDS WITH APPLICATIONS TO WHITE-LIGHT SHEARING INTERFEROMETRY

THESIS

AFIT/GEO/EE/78-1

Paul S. Idell
2nd Lt USAF

DDC
RECEIVED
FEB 12 1979
A

Approved for public release; distribution unlimited.

(14) AFIT/GEO/EE/78-1

(6) COHERENCE PROPERTIES OF BROADBAND OPTICAL FIELDS
WITH APPLICATIONS TO
WHITE-LIGHT SHEARING INTERFEROMETRY.

THESIS

(9) Master's thesis,

Presented to the Faculty of the School of Engineering
of the Air Force Institute of Technology
Air Training Command
in Partial Fulfillment of the
Requirements for the Degree of
Master of Science

(12) 113 p.

(10) by
Paul S. Idell ~~B.S.~~
2nd Lt USAF
Graduate Electro-Optics

(11) ~~December~~ 1978

ACCESSION for
NTIS White Section
DDC Buff Section
UNANNOUNCED
JUSTIFICATION
BY
DISTRIBUTION/AVAILABILITY CODES
DIST. AVAIL. and/or SPECIAL
A

Approved for public release; distribution unlimited.

012 225

slr

PREFACE

And God said, "Let there be light . . . and let it be broadband."

The desire to image distant objects illuminated by naturally occurring (i.e., white) light provided a primary motivation for this work. The analysis of a white-light shearing interferometer necessitated the development of a coherence model which would adequately describe the interference of this so-called "incoherent light." Analysis of the interferometer is presented as an application of the broadband field model developed in Chapter II.

I would like to thank my sponsor Donald W. Hanson, Rome Air Development Center (OCSE), for initially providing me with this interesting problem, and for continuing to support me throughout the study. I also gratefully acknowledge Professors Donn Shankland and Peter Maybeck for serving as readers, and for contributing their comments and constructive criticism to the final draft.

I would like to especially thank Captain Stanley R. Robinson for ably advising me on the thesis, and for providing much appreciated guidance and motivation throughout the study. His interest in the problem, as well as my personal development, had no small part in sustaining my enthusiasm throughout these past months.

Paul S. Idell

Contents

79 01 30 146

List of Figures

List of Tables

ABSTRACT

A free-space propagation model for broadband optical fields is developed based on a Karhunen-Loéve (KL) expansion of the time-varying portion of a coherence separable broadband optical envelope. For long characterization intervals it is found that the eigenfunctions of the KL expansion are approximated by complex exponentials of a Fourier series expansion; the corresponding eigenvalues are approximated by samples of the temporal power spectrum, sampled at the harmonic frequencies of the Fourier series expansion. The resulting modal expansion provides an intuitively simple interpretation of the propagation of broadband fields and allows the output field correlation to be easily calculated.

The propagation model is applied to the analysis of a lateral shear AC interferometer, which has been used to measure the spatial phase variations of a white-light optical field envelope located at its input aperture. It is found that the interferometer's operation for broadband fields causes the phase which is measured by the interferometer to be related to a spatially filtered version of the aperture field. The effect of this spatial filtering on the phase measurement is studied for aperture fields with arbitrary spatial coherence.

Finally, the propagation model is applied to the shearing interferometer's operation as a wavefront sensor in a phase-compensated imaging system, where the phase of the aperture field envelope has been disrupted by atmospheric turbulence. The turbulence-induced phase perturbation is modeled as a unit-modulus phase screen introduced at the aperture plane

of the interferometer for each temporal mode of the field expansion. The space-time separability of the source field allows the visibility effects of extended source distributions on the interferometer's operation to be analyzed separately from the spatial filtering effects of the measurement process due to broadband source emission. The interference fringe visibility is discussed for uniform and complex source radiance distributions, and the interferometer phase measurement is evaluated for typical phase-compensated imaging applications.

COHERENCE PROPERTIES OF BROADBAND OPTICAL FIELDS WITH APPLICATIONS TO WHITE-LIGHT SHEARING INTERFEROMETRY

I. Introduction

Atmospheric turbulence, caused by random fluctuations in the refractive index of air, degrades the imaging capability of ground-based astronomical telescopes. As light from the source propagates down through the atmsophere, turbulence tends to distort the shape of the optical wavefront as well as cause intensity variations across the wavefront (Ref 1:46-48). Intensity variations are caused by a random lensing action and give rise to scintillation and the twinkling of stars. The major effect on image quality, however, is due to the random fluctuations of the optical phasefront. In long-exposure telescopic photography the attainable resolution is turbulence limited, rather than diffraction limited, to about two seconds of arc (Refs 2 and 3).

Recently much interest has developed in the use of predetection phase-compensation for improving the quality of images distorted by atmospheric turbulence (Refs 4, 5, 6, and 7). In the system described by Hardy, et al. (Ref 7), real-time phase-compensation is accomplished by correcting the optical wavefront at the imaging system's input aperture with a monolithic piezoelectric mirror. The wavefront deformation at the input aperture is determined with the use of a lateral shear AC interferometer (Ref 8) which measures the wavefront tilt of the field at several locations in the aperture plane. The operation of this interferometer as a wavefront sensor in atmospheric correction systems is also discussed in Refs 9 and 10.

In addition to atmospheric compensation for imaging applications, there exist other active optic systems for which real-time correction of wavefront aberrations is required (Refs 11, 12, and 13). As a part of these systems, the lateral shear AC interferometer may be used to measure wavefront aberrations introduced by either surface deformations in the optics or fluctuations in the transmission medium. A broad overview of current active optic systems, including descriptions of various wavefront sensors and wavefront correction devices, can be found in Ref 10. Several detailed articles on the current theory and application of active optic systems also appear in the March 1977 issue of the Journal of the Optical Society of America.

At this time the operation of the shearing interferometer mentioned above has been analyzed with respect to its compensated imaging applications and for limited classes of input fields. A description of the interferometer's operation for more general aperture fields is needed. Furthermore, since sources of primary interest in astronomical imaging applications are illuminated with naturally occuring light (e.g., sunlight), the wavefront which must be measured by the interferometer is the wavefront of a white-light (temporally broadband) aperture field. The operation of the shearing interferometer for extended, broadband sources is not well understood.

Problem

The object of this study is to provide a clear and concise explanation of how the lateral shear AC interferometer measures the wavefront slope of a white-light aperture field. The effect of broadband light on

the interferometer phase measurement is to be determined. Of particular interest to its application in compensated imaging systems, a unified, wave-optics description of the interferometer with regard to broadband, extended sources is to be given.

Approach

This paper presents a description of the lateral shear AC interferometer based on a model developed for the free-space propagation of coherence separable, temporally broadband optical fields. By definition, fields which are coherence separable are those whose space-time correlation factors into a product of a spatial correlation and a time correlation. Coherence separability allows the input fields to be simply represented, and lends tractability to the mathematics. However, because the spatial part of a source field represented in this manner is independent of time, attention is restricted to sources which do not move and whose illumination (or luminance) is time-invariant. Sources must also be assumed to be perfectly diffuse (i.e., Lambertian), so that their emission spectrum is not a function of viewing angle.

By temporally broadband it is meant that the source emission spectrum is broad with respect to its mediam wavelength--for the white-light applications which are considered in this paper, the optical fields are assumed to range over the entire visible range, nominally 0.4 to 0.7 μm. The specific functional form of the temporal power spectrum is not specified, although the spectrum is assumed to be smoothly varying over the visible range. The median wavelength of white-light is assumed to be 0.55 μm.

In Chapter II a free-space propagation model for broadband optical fields based on a modal expansion of the time-varying portion of the field is developed. The temporal and spatial variations in the optical field are modeled as complex random processes, where the bandwidth of the stationary time process corresponds to the bandwidth of the visible spectrum. Spatial variations of the input field are assumed to be independent of time so that the space-time field correlations are coherence separable. Using the broadband propagation model, the output field correlation due to broadband source fields is calculated and output field coherence is specialized for sources with special cases of spatial coherence.

The broadband propagation model is applied to the shearing interferometer optics train in Chapter III, and the interferometer output signal for x-shear is determined. To simplify the analysis, diffraction effects due to finite lens size are ignored, all optics are assumed to be perfectly transmissive and aberration-free, and the lenses are assumed to be apochromatic. The phase which is measured by the interferometer is shown to be related to the phase of the spatial part of the complex aperture field envelope. The effects of white-light on the aperture field phase measurement, as derived from the interferometer output signal, are shown for aperture fields with arbitrary spatial coherence.

Finally, in Chapter VI the shearing interferometer phase measurement is determined for an aperture field due to an extended, white-light source viewed through atmospheric turbulence. The source field is assumed to be coherence separable, corresponding to that reflected by a perfectly diffuse, stationary object illuminated by white light. The source is also assumed to be distributed and spatially incoherent as well as being temporally

broadband. The optical phase distortion caused by atmospheric turbulence is modeled as a multiplicative phase factor introduced at the aperture plane of the interferometer for each wavelength. Validity of this model is discussed in detail. Fundamental limitations on interference fringe visibility and phase measurement, due to source radiance distribution and emission spectrum, are discussed.

Functional Notation

This section introduces a standardized set of notation which is used extensively throughout the paper.

Propagation Geometry. All optical fields are defined in planes P_i consisting of points $\bar{r}_i = (x_i, y_i)$ of a right-handed rectangular coordinate system (x,y,z). The propagation of fields is assumed to be in the positive z-direction. Planes and points on them are denoted by a subscript indicating the plane's position on the z-axis. For example, plane P_1 consists of points $\bar{r}_1 = (x_1, y_1)$ for which $z = z_1$. Fields defined in planes are denoted by the subscript identifying the plane, e.g., optical field $U_1(\bar{r}_1, t)$ is located at plane P_1 containing points $\bar{r}_1 = (x_1, y_1)$.

Summation. Unless specifically noted in the text, all summations range over all integers denoted by their index. For example:

$$\sum_n x_n = \sum_{n=-\infty}^{\infty} x_n \tag{1-1}$$

Integrals. All single dimensional integrals are denoted by an integration symbol followed by the differential of the variable being integrated. Two-dimensional integrals are denoted by two integration symbols followed by the differentials of the integration variables.

Integration over a plane containing points $\bar{r}_i = (x_i, y_i)$ may be abbreviated by a single integral sign followed by the differential $d\bar{r}_i = dx_i dy_i$. Unless the limits of integration are explicitly written, the range of integration is doubly-infinite. For example

$$d\bar{r}_1 g(\bar{r}) = \int dx_1 \int dy_1 g(x_1, y_1) \tag{1-2}$$

denotes the doubly-infinite, two-dimensional integral of the function g over points $\bar{r}_1 = (x_1, y_1)$ in plane P_1.

Fourier Transforms. Two-dimensional Fourier transforms are doubly-infinite integrals defined in the following way:

$$F_{xy}\{g(\bar{r})\} = \int d\bar{r}\, g(\bar{r}) \exp[-j2\pi(f_x x + f_y y)] \tag{1-3}$$

where $F_{xy}\{\cdot\}$ denotes the Fourier transform with respect to the variables x and y, where $\bar{r} = (x,y)$; and f_x and f_y are the transform variables associated with x and y, respectively. The inverse Fourier transform is defined in a similar manner:

$$F^{-1}_{f_x f_y}\{g(\bar{f})\} = \int d\bar{f}\, g(\bar{f}) \exp[+j2\pi(f_x x + f_y y)] \tag{1-4}$$

where $F^{-1}_{f_x f_y}\{\cdot\}$ denotes the inverse Fourier transform with respect to variables f_x and f_y, when $\bar{f} = (f_x, f_y)$; and x and y are the space variables associated with the transform variables f_x and f_y, respectively. One-dimensional Fourier and inverse Fourier transforms are defined in a manner similar to that above:

$$F_x\{g(x)\} = \int dx\, g(x) \exp[-j2\pi f x] \tag{1-5}$$

and

$$F^{-1}_f\{g(f)\} = \int df\, g(f) \exp[+j2\pi x f] \tag{1-6}$$

II. COHERENCE PROPERTIES OF BROADBAND OPTICAL FIELDS

In this chapter the spatial coherence properties of broadband optical fields are investigated based on a modal expansion of the time-varying part of the field. Although results presented here are derived for specific application to white-light optical systems in the visible (0.4 to 0.7 μm), the models developed are sufficiently general and may be applied to a wide class of broadband optical and infra-red systems. The input fields are assumed to be coherence separable, and the power spectra of the time-fluctuations are assumed to be smooth over all frequency ranges on the order of T^{-1}, where T is the characterization interval of the temporal process.

Complex Field Envelope

Let $U_1(\bar{r}_1,t)$ represent the complex field envelope of a temporally broadband (white-light) optical field propagating along the positive z-axis. The field is defined in a plane P_1 located at $z = z_1$ containing points $\bar{r}_1 = (x_1,y_1)$. If the temporal fluctuations of the field are centered at optical frequency f_0, the scalar electric field fluctuations of the electro-magnetic field may be written (Refs 14: 494-499; 15:12)

$$E_1(\bar{r}_1,t) = \mathrm{Re}\{U_1(\bar{r}_1,t)\exp[-j2\pi f_0 t]\} \qquad (2\text{-}1)$$

where $E_1(r_1,t)$ is the normalized scalar electric field given in volts per meter per $\sqrt{\text{ohm}}$; Re $\{\cdot\}$ means "the real part of;" and $f_0 = c/\lambda_0$, when c is the speed of light in vacuum, and λ_0 is the median wavelength of the light.

For simplicity of the model, the spatial variations of $U_1(\bar{r}_1,t)$ are assumed to be independent of time, and the field is defined to be coherence separable:

$$U_1(\bar{r}_1,t) = u_1(\bar{r}_1)w(t) \tag{2-2}$$

where $u_1(\bar{r}_1)$ represents the spatial part of the input field and $w(t)$ is the broadband, time-varying portion of the field. Strictly speaking, this coherence model is applicable to source fields whose spatial variations are constant for all time. This restriction can be loosened somewhat for the case where the spatial variations are constant over time intervals comparable to the characterization time T of the temporal process. As a convention $u_1(\bar{r}_1)$ is assigned units volts per meter per $\sqrt{\text{ohm}}$; $w(t)$ is dimensionless.

The spatial and temporal parts of the optical field $u_1(\bar{r}_1)$ and $w(t)$ are assumed to be complex, zero-mean random processes which may be represented in terms of their real and imaginary quadratures as

$$u_1(\bar{r}_1) = u_{1_R}(\bar{r}_1) + ju_{1_I}(\bar{r}_1) \tag{2-3}$$

and

$$w(t) = w_R(t) + jw_I(t) \tag{2-4}$$

where $u_{1_R}(\bar{r}_1)$ and $u_{1_I}(\bar{r}_1)$ are the real and imaginary parts, respectively, of the complex random process $u_1(\bar{r}_1)$; and $w_R(t)$ and $w_I(t)$ are the real and imaginary parts of $w(t)$. If $u_1(\bar{r}_1)$ is assumed to have identically distributed, but uncorrelated quadratures, the second moments of $u_1(\bar{r}_1)$ may be written

$$\left\langle u_1(\bar{r}_1)u^*(\bar{r}_1')\right\rangle = R_1(\bar{r}_1,\bar{r}_1') \tag{2-5}$$

and

$$\left\langle u_1(\bar{r}_1)u_1(\bar{r}_1')\right\rangle = 0 \tag{2-6}$$

where $R_1(\bar{r}_1,\bar{r}_1')$ is called the spatial correlation function, $\langle\cdot\rangle$ denotes an ensemble average, and * denotes the complex conjugate. Similarly, if $w_R(t)$ and $w_I(t)$ are assumed to be identically distributed and uncorrelated, the second moments of the complex random process $w(t)$ are

$$\left\langle w(t)w^*(t')\right\rangle = R_w(t,t') \tag{2-7}$$

$$\left\langle w(t)w(t')\right\rangle = 0 \tag{2-8}$$

Since the exact form of the spatial or temporal parts of the input field are not known, it is reasonable to model them as complex random processes--if for no other reason than a lack of better information. Also, since for any naturally occurring phenomenon it would seem unreasonable to assume that one quadrature should take precidence over the other, the random processes are assumed to have identically distributed quadratures.

Furthermore, if $w(t)$ is assumed to be stationary, the correlation of the temporal fluctuations of the field may be written

$$R_w(t,t') = R_w(t-t') = R_w(\tau) \tag{2-9}$$

$$R_w(\tau) = F_f^{-1}\{S_w(f)\} \tag{2-10}$$

where $\tau = t - t'$, $F_f^{-1}\{\cdot\}$ denotes the inverse Fourier transform with respect to f, and $S_w(f)$ is twice the power spectrum of either $w_R(t)$ or $w_I(t)$. Henceforth, the temporal correlation is assumed to be stationary as defined by Eq (2-9). The space-time correlation or mutual

correlation function of the broadband field $U_1(\bar{r}_1,t)$ is defined as

$$\Gamma_1(\bar{r}_1,\bar{r}_1',t,t') = \left\langle U_1(\bar{r}_1,t)U_1^*(\bar{r}_1',t')\right\rangle \tag{2-11}$$

$$= \left\langle U_1(\bar{r}_1)u_1^*(\bar{r}_1')\right\rangle \left\langle w(t)w^*(t')\right\rangle \tag{2-12}$$

$$= R_1(\bar{r}_1,\bar{r}_1')R_w(\tau) \tag{2-13}$$

Therefore, the space-time correlation of a coherence separable field factors as the product of the spatial correlation function and the temporal correlation of the field.

For typical white-light applications, the spectral content of $w(t)$ may be considered to range between 0.4 and 0.7 μm, corresponding to a temporal bandwidth Δf equal to 3×10^{14} Hertz. For convenience, the power spectrum $S_w(f)$ will be normalized, so that

$$\int df S_w(f) = 1 \tag{2-14}$$

Thus, all the power in the complex field is assigned to the spatial part of the field envelope $u_1(\bar{r}_1)$. A representative broadband power spectrum $S_w(f)$ and its corresponding correlation function $R_w(\tau)$ are sketched in Figure 1, where B is the nominal temporal bandwidth defined by

$$B = \frac{1}{2}\Delta f \tag{2-15}$$

the coherence time of the complex temporal process is approximately given by $\tau_c \approx \frac{1}{B}$.

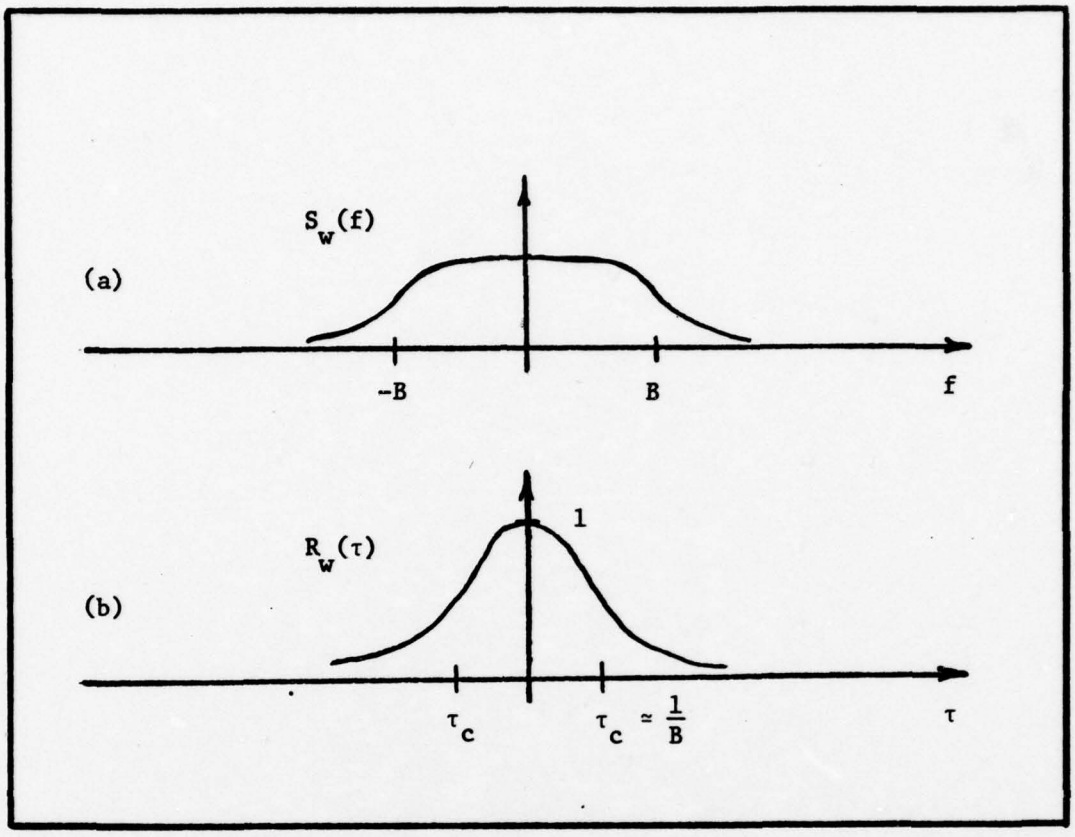

Figure 1. (a) A Typical Broadband Temporal Power Spectrum $S_w(f)$ and (b) Its Corresponding Correlation Function $R_w(\tau)$

Modal Expansion of Complex Field Envelope

In this section a modal expansion of the time-varying portion of the complex field envelope $w(t)$ is developed. A Karhunen-Loéve (KL) expansion is used so that the coefficients of the expansion are uncorrelated over the characterization interval. For long characterization times, it is shown that the basis functions of the KL expansion can be approximated by complex exponentials, providing an intuitively simple interpretation of the propagation of broadband fields.

Modal Expansion of $w(t)$. Consider the following modal expansion of the complex random process $w(t)$ along a complete orthonormal (CON) set of basis functions $\{\phi_n(t)\}$ over a finite time interval $[-\frac{T}{2}, \frac{T}{2}]$:

$$w(t) = \underset{N\to\infty}{\text{l.i.m.}} \sum_{n=-N}^{N} w_n \phi_n(t)$$

$$\text{for } -\frac{T}{2} < t < \frac{T}{2} \tag{2-16}$$

$$\text{where } w_n = \frac{1}{T} \int_{-\frac{T}{2}}^{\frac{T}{2}} dt\, w(t)\phi_n^*(t) \tag{2-17}$$

"l.i.m." denotes limit in the mean, implying a mean-square convergence of the sum (2-16), and n is the integer index of the n^{th} temporal mode. Note that $\{\phi_n(t)\}$ is a set of complex functions yet to be specified. Also, since $w(t)$ is assumed to be a zero-mean, complex random process $\{w_n\}$ are zero-mean, complex random variables.

By proper selection of basis functions $\{\phi_n(t)\}$ it is possible to expand $w(t)$ so that the coefficients of the expansion $\{w_n\}$ are pairwise uncorrelated:

$$\langle w_n w_{n'}^* \rangle = \langle w_n \rangle \langle w_{n'} \rangle = 0 \tag{2-18}$$

for $n \neq n'$. The second equality comes about because the coefficients are zero-mean random variables.

A necessary and sufficient condition for the $\{w_n\}$ to be uncorrelated is that the basis functions $\{\phi_n(t)\}$ are the solutions to the Fredholm equation (Ref 16:180):

$$\gamma_n \phi_n(t) = \int_{-\frac{T}{2}}^{\frac{T}{2}} dt' \, R_w(t,t') \, \phi_n(t')$$

for $-\frac{T}{2} < t < \frac{T}{2}$ (2-19)

where $\{\gamma_n\}$ are the real eigenvalues associated with the eigenfunctions $\{\phi_n(t)\}$ for all integers $n : -\infty < n < \infty$. The expansion of $w(t)$ on a CON set of eigenfunctions over an interval yielding uncorrelated coefficient is known as a Karhunen-Loéve (KL) expansion. If the basis functions $\{\phi_n(t)\}$ of (2-16) are solutions to (2-19) then the modal expansion of $w(t)$ is such an expansion.

Results from linear integral equation theory (Refs 17:122-140; 18:242-246) state that any square integrable kernel $R_w(t,t')$ of (2-19) may be expanded in a series

$$R_w(t,t') = \sum_n \gamma_n \phi_n(t) \, \phi_n^*(t')$$

for $-\frac{T}{2} < t,t' < \frac{T}{2}$ (2-20)

where the convergence is uniform for $-\frac{T}{2} < t,t' < \frac{T}{2}$. Eq (2-20) is called Mercer's theorem. It can be shown (Ref 15:409) that if the correlation function of a zero-mean, complex random process $w(t)$ can be expanded in a form (2-20), the modal expansion given in (2-16) will converge in mean-square. Thus, for any correlation $R_w(t,t')$ which is continuous and bounded for $-\frac{T}{2} < t,t' < \frac{T}{2}$, the modal expansion of $w(t)$ given in (2-16) will converge in mean-square to the process $w(t)$.

Eigenfunctions and Eigenvalues for Long T. For stationary random processes characterized over long time intervals $[-\frac{T}{2}, \frac{T}{2}]$, it can be shown (Ref 16:205-207) that the eigenfunctions $\{\phi_n(t)\}$ and associated

eigenvalues $\{\gamma_n\}$ which are solutions to the Fredholm equation (2-19) can be approximated by

$$\phi_n(t) = \exp[+j2\pi \frac{n}{T} t]$$

for $-\frac{T}{2} < t < \frac{T}{2}$ (2-21)

and $$\gamma_n = \frac{1}{T} S_w(\frac{n}{T}) \quad (2\text{-}22)$$

where T is the characterization interval in seconds and $S_w(\frac{n}{T})$ is the power spectrum of the complex random process $w(t)$, defined in Eq (2-10), sampled at frequencies $\frac{n}{T}$ Hertz.

The magnitude of T needed for the validity of the approximation depends on how quickly $S_w(f)$ changes near frequency $f = \frac{n}{T}$. For smooth spectra, long T means long compared to the reciprocal bandwidth of the fluctuations of the optical envelope:

$$T >> \frac{1}{B} \quad (2\text{-}23)$$

For white-light applications the bandwidth $B \simeq 1.5 \times 10^{14}$ Hertz. Therefore, for a characterization time T much greater than 6.67×10^{-13} seconds, the $\{\phi_n(t)\}$ of the expansion over time interval of length T become the complex exponentials of a Fourier series expansion, and the eigenvalues $\{\gamma_n\}$ corresponding to the eigenfunctions become samples of the power spectrum $S_w(f)$ evaluated at the harmonic frequencies of the Fourier series expansion.

Thus, for long characterization time T, the eigenfunctions of the KL (modal) expansion (2-16) may be approximated by complex exponentials,

and the expansion for $w(t)$ becomes

$$w(t) = \sum_n w_n \, e^{+j2\pi \frac{n}{T} t}$$

for $-\frac{T}{2} < t < \frac{T}{2}$ (2-24)

where $$w_n = \frac{1}{T} \int_{-\frac{T}{2}}^{\frac{T}{2}} dt \; w(t) e^{-j2\pi \frac{n}{T} t} \tag{2-25}$$

and the statistics of the process $w(t)$ are such that the sum is assumed to converge in mean-square as discussed earlier.

With regard to the above approximation, it may be noted that if the random process is expanded in a Fourier series, it can be shown (Ref 19:94) that the coefficients of the expansion $\{w_n\}$ become uncorrelated as the expansion interval T gets long.

Eigenvalue Statistics. The expected value of the energy of $w(t)$ in time interval $[-\frac{T}{2}, \frac{T}{2}]$ is defined

$$E_T = \left\langle \int_{-\frac{T}{2}}^{\frac{T}{2}} dt \; w(t) w^*(t) \right\rangle \tag{2-26}$$

$$= T \sum_n \left\langle w_n w_n^* \right\rangle \tag{2-27}$$

where the modal expansion for $w(t)$ has been used. Using Mercer's theorem (2-20), the mean energy of the process for long characterization time T is

$$E_T = \sum_n S_w(\tfrac{n}{T}) \tag{2-28}$$

Equating each term of sums (2-27) and (2-28) and using Eq (2-18) yields

$$\left\langle w_n w_{n'}^* \right\rangle = \frac{1}{T} S_w(\tfrac{n}{T}) \, \delta_{nn'} \tag{2-29}$$

where $\delta_{nn'}$ is a Kronecker delta. Thus, for long characterization intervals, the mean-square value of each expansion coefficient $\{w_n\}$ is seen to be just a sample of the temporal power spectrum evaluated at the coefficient's harmonic frequency.

Modal Expansion of the Optical Envelope. From Eqs (2-2) and (2-24), the complex field envelope of a coherence separable, temporarily broadband optical field in a plane $z = z_1$ can be written

$$U_1(\bar{r}_1,t) = \sum_n u(\bar{r}_1)\, w_n e^{+j2\pi \frac{n}{T} t}$$

for $-\frac{T}{2} < t < \frac{T}{2}$ (2-30)

where the complex field envelope is taken with respect to a carrier at optical frequency f_0, as in (2-1). Furthermore, its mutual correlation function can be written

$$\Gamma_1(\bar{r}_1,\bar{r}_1',t,t') = \left\langle U(\bar{r}_1,t) U_1^*(\bar{r}_1',t') \right\rangle \quad (2\text{-}31)$$

$$= \sum_n \sum_{n'} \left\langle w_n w_{n'}^* \right\rangle \left\langle u_1(\bar{r}_1) u_1^*(\bar{r}_1') \right\rangle$$

$$\exp\left[j \frac{2\pi}{T} (nt - n't')\right] \quad (2\text{-}32)$$

for $-\frac{T}{2} < T < \frac{T}{2}$. Note that the modal expansion of $w(t)$ allows the ensemble average over time sample functions in the temporal correlation to be replaced by a sum of expected values of random variables.

Since the modal expansion coefficients have been chosen so as to be pairwise uncorrelated (Ref Eq (2-29)), Eq (3-32) may be further simplified:

$$\Gamma_1(\bar{r}_1,\bar{r}_1',t,t') = \sum_n \frac{1}{T} S_w\left(\frac{n}{T}\right) R_1(\bar{r}_1,\bar{r}_1') \exp\left[j2\pi \frac{n}{T}(t - t')\right]$$

for $-\frac{T}{2} < t < \frac{T}{2}$. (2-33)

The n^{th} temporal mode of the optical envelope is defined by the n^{th} term in the series (2-30)

$$U_{l_n}(\bar{r}_1,t) = u_1(\bar{r}_1)w_n e^{+j2\pi\frac{n}{T}t}$$

$$\text{for } -\frac{T}{2} < t < \frac{T}{2} \qquad (2\text{-}34)$$

where $U_{l_n}(\bar{r}_1,t)$ is the baseband representation of a monochromatic optical field at frequency $f_n = (f_0 - \frac{n}{T})$; $u_1(\bar{r}_1)$ is the wavelength-independent spatial part of the complex field; and $\{w_n\}$ is the n^{th} coefficient of the modal expansion for $w(t)$ defined in Eq (2-25).

The importance of the modal expansion for the complex field envelope given in Eq (2-30) is the following. Since Maxwell's equations governing propagation of electromagnetic waves for homogeneous, isotropic media are linear in space and time, each n^{th} term in the expansion--or, n^{th} temporal mode--propagates individually. In terms of optical fields this means that each temporal mode may be propagated as a monochromatic wave at frequency $f_n = f_0 - \frac{n}{T}$. By superposition, the output broadband field is simply the sum of all the individually propagated modes.

The free-space propagation of broadband optical fields using the modal expansion developed above is discussed in the next section.

Free-Space Propagation Model for Broadband Optical Fields

Consider two parallel planes P_1 and P_2 separated by a free-space propagation path of length Z as shown in Figure 2. The propagation of monochromatic fields from input plane P_1 at $z = z_1$ to output plane P_2 at $z = z_2$ is governed by the Huygens-Fresnel integral (Ref 20:60) which may be written

$$u_2(\bar{r}_2) = \frac{e^{jk_0Z}}{j\lambda_0 Z} \int d\bar{r}_1 u_1(\bar{r}_1) \exp[j\frac{k_0}{2Z}|\bar{r}_2-\bar{r}_1|^2] \qquad (2\text{-}35)$$

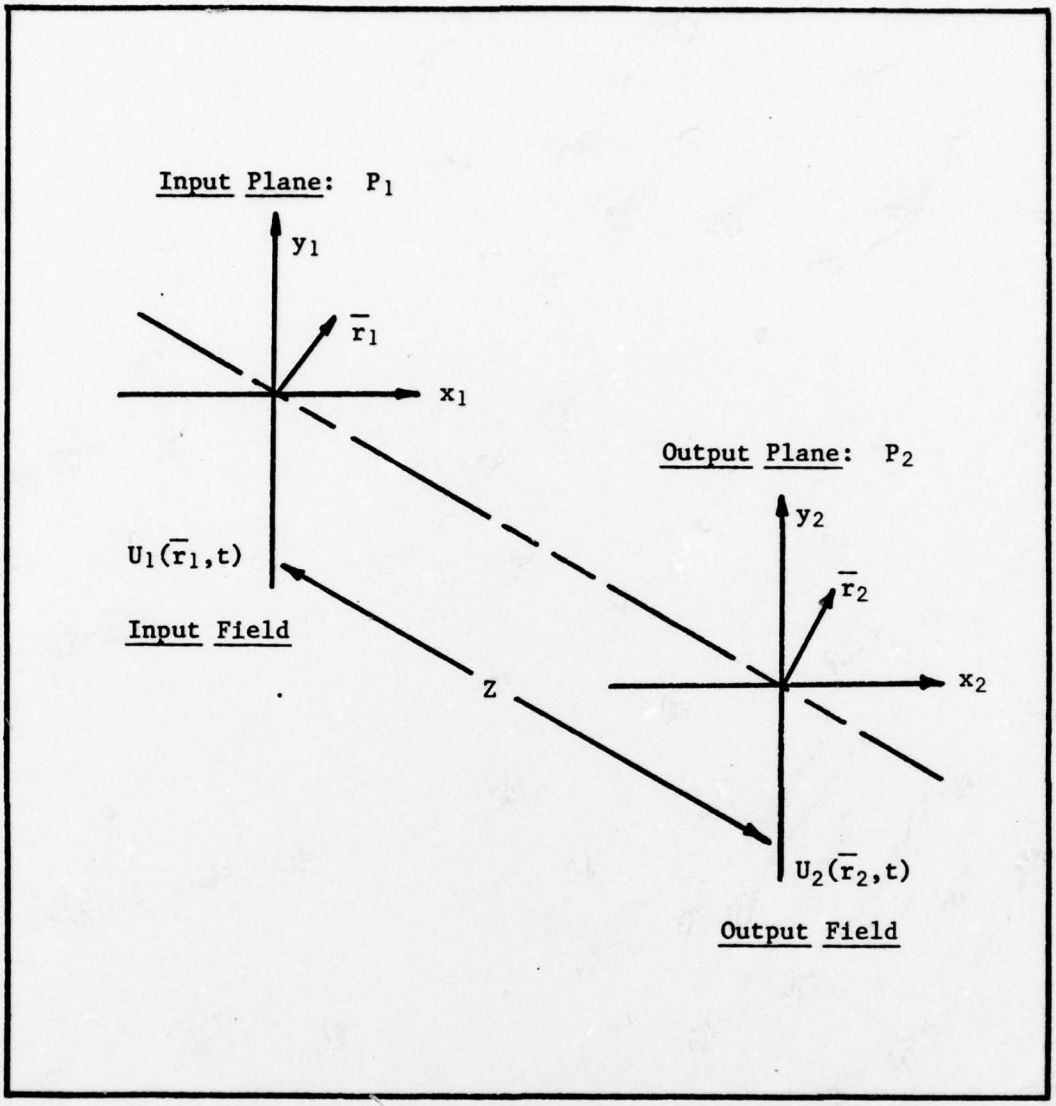

Figure 2. Free-Space Propagation Geometry

where $u_1(\bar{r}_1)$ is the complex field amplitude of the input field, $u_2(\bar{r}_2)$ is the field amplitude of the output field, $\bar{r}_1 = (x_1,y_1)$ is located in P_1, $\bar{r}_2 = (x_2,y_2)$ is located in P_2, $k_0 = \frac{2\pi}{\lambda_0}$, λ_0 is the wavelength of the light and $Z = z_2 - z_1$ is the distance from plane P_1 to P_2 in meters.

In Eq (2-35) the paraxial (Fresnel) approximation has been used. For many applications, the optical fields of interest are confined to a region about the z-axis whose maximum linear dimension is small compared to the propagation distance Z. For these situations, the Fresnel approximation to the Huygens-Fresnel integral is very good. This form also allows the computations associated with wave propagation and diffraction to be greatly simplified, allowing a "systems" type representation of these effects.

For a monochromatic field of wavelength λ_n the Huygens-Fresnel integral (2-35) can be rewritten

$$u_{2_n}(\bar{r}_2) = \frac{e^{jk_nZ}}{j\lambda_nZ} \int d\bar{r}_1 \; u_{1_n}(\bar{r}_1) \exp[j\frac{k_n}{2Z}|\bar{r}_2-\bar{r}_1|^2] \tag{2-36}$$

where $$k_n = \frac{2\pi}{\lambda_n} \tag{2-37}$$

and $u_{1_n}(\bar{r}_1)$ and $u_{2_n}(\bar{r}_2)$ represent the complex input and output field amplitudes at wavelength λ_n.

Using the modal expansion for a temporally broadband optical field given in Eq (2-30), the output field mode $U_{2_n}(\bar{r}_2,t)$ due to a monochromatic temporal mode at optical frequency $f_n = \frac{c}{\lambda_n} = f_0 - \frac{n}{T}$ at the input plane can be written

$$U_{2_n}(\bar{r}_2,t) = \frac{e^{jk_nZ}}{j\lambda_nZ} \int d\bar{r}_1 \; U_{1_n}(\bar{r}_1,t) \exp[j\frac{k_n}{2Z}|\bar{r}_2-\bar{r}_1|^2]$$

for $-\frac{T}{2} < t < \frac{T}{2}$ (2-38)

where $$\lambda_n = \lambda_0 \, \xi^{-1}(n) \tag{2-39}$$

$$k_n = \frac{2\pi}{\lambda_n} = \frac{2\pi}{\lambda_0} \, \xi(n) \tag{2-40}$$

$$\xi(n) = 1 - \frac{n}{f_0 T} \tag{2-41}$$

and $U_{1_n}(\bar{r}_1,t)$ is the n^{th} temporal mode of broadband field envelope $U_1(\bar{r}_1,t)$ located at plane P_1 given previously in Eq (2-34).

Note that both input and output field modes are baseband representations of the n^{th} temporal mode at the input and output planes, respectively, taken with respect to an optical carrier at center frequency $f_0 = \frac{c}{\lambda_0}$.

For broadband (white-light) fields, the output field $U_2(\bar{r}_2,t)$ can be written as the sum of the individually propagated temporal modes:

$$U_2(\bar{r}_2,t) = \sum_n U_{2_n}(\bar{r}_2,t)$$

for $-\frac{T}{2} < t < \frac{T}{2}$ (2-42)

where $U_{2_n}(\bar{r}_2,t)$ is given in Eq (2-38) and the sum converges in the mean. For reference, Eq (2-42) is called the free-space propagation model for temporally broadband optical fields.

Field Coherence Properties of Broadband Sources

The purpose of this section is to calculate the correlation of an optical field at an output plane due to a temporally broadband source with arbitrary spatial coherence. First, the output field correlation is calculated using the broadband field propagation model developed in the

previous section. Using statistical models for the spatial coherence of the source, results for the spatial correlation of the output field are derived for spatially coherent and incoherent sources. Results for the spatial correlation of broadband light, derived using the broadband field propagation model, are compared to well-known results for quasi-monochromatic fields.

Output Field Correlation. The source field, defined in plane P_1, is assumed to be coherence separable so that the input field envelope may be written as in Eq (2-30):

$$U_1(\bar{r}_1,t) = \sum_n u_1(\bar{r}_1) w_n e^{+j2\pi \frac{n}{T} t} \tag{2-43}$$

where $u_1(\bar{r}_1)$ represents the spatial part of the complex field and the modal expansion for temporally broadband (white-light) fields has been used.

Using the broadband field propagation results given in Eq (2-42), the output field at plane P_2 due to a temporally broadband optical field at P_1 is

$$U_2(\bar{r}_2,t) = \sum_n \frac{e^{jk_n Z}}{j\lambda_n Z} w_n \exp[j2\pi \tfrac{n}{T} t] \int d\bar{r}_1 \, u_1(\bar{r}_1) \exp[j \tfrac{k_n}{2Z} |\bar{r}_2 - \bar{r}_1|^2] \tag{2-44}$$

where Z is the distance between planes P_1 and P_2 in meters.

The correlation of the broadband output field can be written

$$\Gamma_2(\bar{r}_2,\bar{r}_2',t,t') = \left\langle U_2(\bar{r}_2,t)U_2^*(\bar{r}_2',t')\right\rangle \tag{2-45}$$

$$= \sum_n (\lambda_n Z)^{-2}\frac{1}{T}\, S_w(\tfrac{n}{T})\exp[j2\pi\tfrac{n}{T}(t-t')]$$
$$\int d\bar{r}_1 \int d\bar{r}_1'\, R_1(\bar{r}_1,\bar{r}_1')$$
$$\exp[j\tfrac{k_n}{2Z}(|\bar{r}_2-\bar{r}_1|^2-|\bar{r}_2'-\bar{r}_1'|^2)] \tag{2-46}$$

$$= \sum_n (\lambda_n Z)^{-2}\int d\bar{r}_1 \int d\bar{r}_1'\, \Gamma_{1_n}(\bar{r}_1,\bar{r}_1',t-t')$$

for $-\frac{T}{2} < t < \frac{T}{2}$
$$\exp[j\tfrac{k_n}{2Z}(|\bar{r}_2-\bar{r}_1|^2-|\bar{r}_2'-\bar{r}_1'|^2)] \tag{2-47}$$

where

$$\Gamma_{1_n}(\bar{r}_1,\bar{r}_1',\tau) = \frac{1}{T}\, S_w(\tfrac{n}{T})R_1(\bar{r}_1,\bar{r}_1')\exp[j2\pi\tfrac{n}{T}\,t\,] \tag{2-48}$$

is the n^{th} temporal mode of the correlation of the source field given in Eq (2-33). The output field correlation $\Gamma_2(\bar{r}_2,\bar{r}_2',t,t')$ or the mutual correlation function expresses the mutual coherence of light fluctuations at points $\bar{r}_2$ and $\bar{r}_2'$ in the output plane, where the fluctuations at $\bar{r}_2$ are taken at time t, and those at $\bar{r}_2'$ are taken at time t'.

Spatial Correlation of Output Field. The spatial correlation of the output field is calculated from Eq (2-47) when $t - t' = \tau = 0$:

$$\Gamma_2(\bar{r}_2,\bar{r}_2') \triangleq \Gamma_2(\bar{r}_2,\bar{r}_2',\tau=0) \tag{2-49}$$

$$= \sum_n (\lambda_n Z)^{-2}\int d\bar{r}_1 \int d\bar{r}_1'\, \Gamma_{1_n}(\bar{r}_1,\bar{r}_1')$$
$$\exp[j\tfrac{k_n}{2Z}\,(|\bar{r}_2-\bar{r}_1|^2-|\bar{r}_2'-\bar{r}_1'|^2)]$$

for $-\frac{T}{2} < t < \frac{T}{2}$ (2-50)

where

$$\Gamma_{1_n}(\bar{r}_1,\bar{r}_1') \triangleq \Gamma_{1_n}(\bar{r}_1,\bar{r}_1',\tau=0) \tag{2-51}$$

$$= \frac{1}{T} S_w(\tfrac{n}{T})\ R_1(\bar{r}_1,\bar{r}_1') \tag{2-52}$$

The output spatial correlation function $\Gamma_2(\bar{r}_2,\bar{r}_2')$ is also called mutual intensity (Ref 14:508-510) of the output field. It expresses the <u>spatial coherence</u> of light at two points $\bar{r}_2$ and $\bar{r}_2'$ in the output plane when both points are considered at the same time. For white-light sources Eq (2-50) is directly related to the fringe visibility of a Michelson stellar interferometer (Ref 22:30) for extended, white-light sources with arbitrary coherence properties.

Let the correlation of the spatial part of the source field be written

$$R_1(\bar{r}_1,\bar{r}_1') = \tilde{\mu}_1(\bar{r}_1,\bar{r}_1')u_1(\bar{r}_1)u_1^*(\bar{r}_1') \tag{2-53}$$

where $\tilde{\mu}_1(\bar{r}_1,\bar{r}_1')$ is defined to be the complex degree of coherence of the source, such that spatially <u>coherent</u> sources are defined as those for

$$\tilde{\mu}_1(\bar{r}_1,\bar{r}_1') = 1 \tag{2-54}$$

spatially <u>incoherent</u> sources are defined so that

$$\tilde{\mu}_1(\bar{r}_1,\bar{r}_1') = \delta(\bar{r}_1-\bar{r}_1') \tag{2-55}$$

Using Eq (2-53) for spatially coherent but temporally broadband sources, the spatial correlation of the output field may be written from Eq (2-50):

$$\Gamma_2(\bar{r}_2,\bar{r}_2') \Big|_{\text{source}}^{\text{coherent}}$$

$$= \sum_n (\lambda_n Z)^{-2} \frac{1}{T} S_w(\frac{n}{T})$$

$$\int d\bar{r}_1 \; u_1(\bar{r}_1) \exp[j \frac{k_n}{2Z} |\bar{r}_2 - \bar{r}_1|^2]$$

$$\int d\bar{r}_1' \; u_1^*(\bar{r}_1') \exp[-j \frac{k_n}{2Z} |\bar{r}_2' - \bar{r}_1'|^2]$$

for $-\frac{T}{2} < t < \frac{T}{2}$. (2-56)

For broadband, spatially incoherent sources Eq (2-50) becomes

$$\Gamma_2(r_2,r_2') \Big|_{\text{source}}^{\text{incoherent}}$$

$$= \sum_n (\lambda_n Z)^{-2} \frac{1}{T} S_w(\frac{n}{T})$$

$$e^{j\psi_n} \int d\bar{r}_1 \; I_1(\bar{r}_1) \exp[-j \frac{k_n}{2Z} \; \bar{r}_1 \cdot (\bar{r}_2 - \bar{r}_2')]$$

for $-\frac{T}{2} < t < \frac{T}{2}$ (2-57)

where $$\psi_n = \frac{k_n}{2Z} (|\bar{r}_2|^2 - |\bar{r}_2'|^2) \tag{2-58}$$

and $$I_1(\bar{r}_1) = u_1(\bar{r}_1) u_1^*(\bar{r}_1) \tag{2-59}$$

is defined to be the intensity of the source in watts per meter squared. Note that Eq (2-57) is an extension of the Van Cittert-Zernicke theorem (Ref 14:508-511) for temporally broadband sources.

In particular, if the source is radiating quasi-monochromatic light at wavelength λ_0 , the temporal power spectrum may be approximated by

$$S_w(\frac{n}{T}) = T \; \delta(n-0) \tag{2-60}$$

and Eq (2-57) yields the mutual intensity for an extended, incoherent, quasi-monochromatic source derived by Born and Wolf (Ref 14:509):

$$\Gamma_2(\bar{r}_2,\bar{r}_2') \Big|_{\substack{\text{quasi-monochromatic,}\\ \text{incoherent source}}} = (\lambda_0 Z)^{-2}\, e^{j\psi_0} \int d\bar{r}_1\, I_1(\bar{r}_1) \exp\left[-j\frac{k_0}{Z}\,\bar{r}_1\cdot(\bar{r}_2-\bar{r}_2')\right] \tag{2-61}$$

where

$$\psi_0 = \frac{\pi}{\lambda_0 Z}\left(|\bar{r}_2|^2-|\bar{r}_2'|^2\right) \tag{2-62}$$

and λ_0 is the median wavelength of the source radiation.

Note that for each temporal mode n the mutual intensity of the light at the output plane is just as prescribed by the Van Cittert-Zernicke theorem. The spatial correlation for white-light, extended sources (2-57) is, therefore, the sum of all the mutual intensities for each temporal mode. Also, since the spatial variations of the source field are assumed to be wavelength-independent, the contribution from each temporal mode is weighted by the temporal power spectrum $S_w(f)$ evaluated at the appropriate harmonic frequency.

Coherence Length for Broadband Optical Fields

Bringing the sum over temporal modes inside the integrals over $\bar{r}_1$ and writing

$$k_n = k_0 + \frac{k_0 n}{f_0 T} \tag{2-63}$$

allows Eq (2-50) to be rewritten in the following form:

$$\Gamma_2(\bar{r}_2,\bar{r}_2') = (\lambda_0 Z)^{-2} \int d\bar{r}_1 \int d\bar{r}_1' \; R_1(\bar{r}_1,\bar{r}_1')$$

$$\hat{R}_w \; \frac{1}{2Zc} \left(|\bar{r}_2-\bar{r}_1|^2-|\bar{r}_2'-\bar{r}_1'|^2\right)$$

$$\exp\left[j \frac{k_0}{2Z} \left(|\bar{r}_2- \bar{r}_1|^2- \bar{r}_2'-\bar{r}_1'|^2\right)\right]$$

for $-\frac{T}{2} < t < \frac{T}{2}$ (2-64)

where

$$\hat{R}_w(\tau) = \frac{1}{T} \sum_n \xi^2(n) S_w\left(\frac{n}{T}\right) \exp\left[-j2\pi\tau\left(\frac{n}{T}\right)\right] \tag{2-65}$$

For wide process bandwidth B and long characterization time T, the sum over temporal modes may be approximated by an integral over v (Ref 16:207):

$$\hat{R}_w(\tau) \simeq \int dv \; \xi^2(v) S_w(v) \exp[-j2\pi\tau v] \tag{2-66}$$

$$= F_v\{\xi^2(v) S_w(v)\} \tag{2-67}$$

where $\xi(v) = \left(1 - \frac{v}{f_0}\right)$ and v has been substituted for $\frac{n}{T}$ as the integration variable.

Eq (2-64) indicates that the spatial correlation of a broadband field can be calculated from a two-fold spatial integral over (1) the spatial correlation of the source $R_1(\bar{r}_1,\bar{r}_1')$ and (2) the contribution from differential path delays of all the temporal modes, written as $R_w(\cdot)$. As shown in Eq (2-67) the differential path contribution to the spatial correlation can be approximated by the Fourier transform of a weighted power spectrum. The relationship of the quadratic term $\xi^2(v)$ to a typical power spectrum is shown in Figure 3.

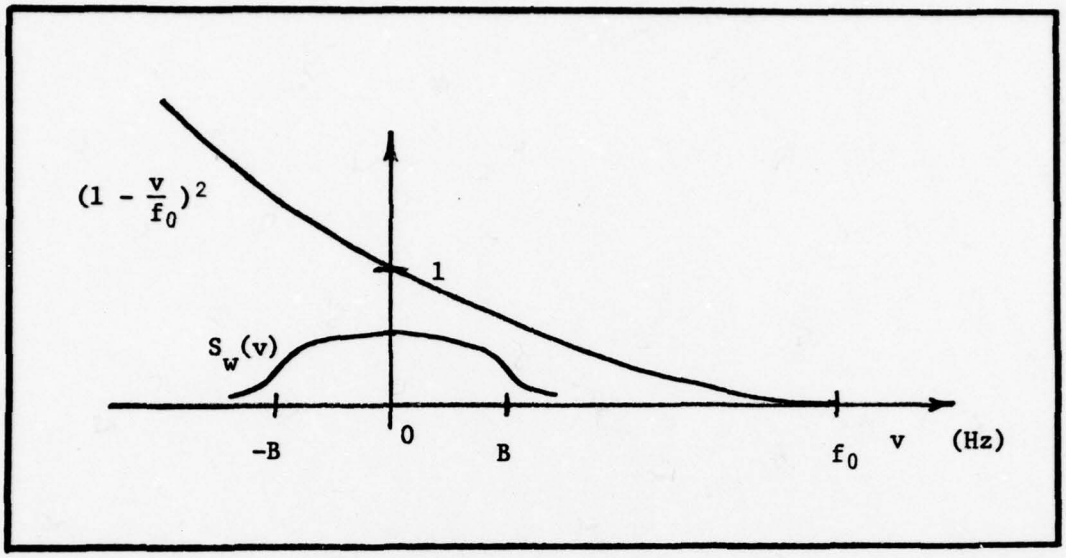

Figure 3. Relationship Between Quadratic Term $\xi^2(v)$ and the Temporal Power Spectrum $S_w(v)$

Expanding

$$\xi^2(v) = 1 - \frac{2v}{f_0} + (\frac{v}{f_0})^2 \qquad (2\text{-}68)$$

and using the differentiation theorem for Fourier transforms (Ref 23:36), $R_w(\tau)$ may be written in terms of the first two derivatives of the temporal correlation function $R_w(\tau)$:

$$\hat{R}_w(\tau) = R_w(\tau) - \frac{2}{j2\pi f_0} \cdot \frac{\partial}{\partial \tau} R_w(\tau) + \frac{1}{(jw\pi f_0)^2} \cdot \frac{\partial^2}{\partial \tau^2} R_w(\tau) \qquad (2\text{-}69)$$

$$= R_w(\tau) + \frac{j}{\pi f_0} \cdot \frac{\partial}{\partial \tau} R_w(\tau) - \frac{1}{(2\pi f_0)^2} \cdot \frac{\partial^2}{\partial \tau^2} R_w(\tau) \qquad (2\text{-}70)$$

where the correlation of the stationary, wideband process $w(t)$ is given by Eq (2-10). If the bandwidth B of $S_w(f)$ is narrow enough so that

$$\frac{n}{T} << f_0 \qquad (2\text{-}71)$$

for all temporal modes with significant energy, then $\xi^2(v) \simeq 1$, and

$$\hat{R}_w(\tau) \simeq R_w(\tau) \tag{2-72}$$

because the correlation functions considered here are even

$$F_v\{S_w(v)\} = F_v^{-1}\{S_w(v)\} = R_w(\tau) \tag{2-73}$$

For any wideband power spectrum of practical interest $R_w(\tau)$ tends to drop off in magnitude for increasing argument (see Figure 1). This tendency will cause a "windowing" effect in the integral (2-64). In terms of spatial coherence, there exists regions in P_1 (consisting of points $\bar{r}_1$ and $\bar{r}_1'$) and P_2 (consisting of points $\bar{r}_2$ and $\bar{r}_2'$) for which the spatial correlation function $\Gamma_2(\bar{r}_2,\bar{r}_2')$ is negligible. If the spatial correlation of the source is stationary for all separations $|\bar{r}_1-\bar{r}_1'|$ in the source plane, the output coherence $\Gamma_2(\bar{r}_2,\bar{r}_2')$ is also stationary and may be written $\Gamma_2(|\bar{r}_2-\bar{r}_2'|)$. The separation $\rho_c = |\bar{r}_2-\bar{r}_2'|$ for which the output correlation function has significant value is called the coherence distance.

Let the spatial correlation of the source be modeled as in Eq (2-53) and assume the complex degree of coherence of the source $\tilde{\mu}_1$ is stationary in spatial coordinates (homogeneous)

$$R_1(\bar{r}_1,\bar{r}_1') = \tilde{\mu}_1(\rho_1)u_1(\bar{r}_1)u_1^*(\bar{r}_1') \tag{2-74}$$

where

$$\rho_1 = |\bar{r}_1-\bar{r}_1'| \tag{2-75}$$

The spatial correlation of the field $U_2(\bar{r}_2,t)$ can then be written

$$\Gamma_2(\bar{r}_2,\bar{r}_2') = (\lambda_0 Z)^{-2} \int d\bar{r}_1 \int d\bar{r}_1' \; \tilde{\mu}_1(\rho_1) u_1(\bar{r}_1) u_1^*(\bar{r}_1')$$

$$\hat{R}_w\left[\frac{1}{2Z_c}\left(|\bar{r}_2-\bar{r}_1|^2-|\bar{r}_2'-\bar{r}_1'|^2\right)\right]$$

$$\exp\left[j\,\frac{k_0}{2Z}\left(|\bar{r}_2-\bar{r}_1|^2-|\bar{r}_2'-\bar{r}_1'|^2\right)\right]$$

for $-\frac{T}{2} < t < \frac{T}{2}$. (2-76)

Special cases of the output spatial correlation function for source fields having various combinations of emission spectra and spatial coherence are given in Table I. Monochromatic fields are assumed to have impulsive emission spectra as given in Eq (2-60). The spatial coherence of coherent and incoherent sources are modeled by Eqs (2-54) and (2-55), respectively.

In summary, it must be noted that the output field correlations listed in Table I are calculated for source fields which are assumed to be coherence separable. Source fields which can be represented in this manner are restricted to those emitted by a perfectly diffuse and stationary object whose spatial characteristics are independent of time. Furthermore, since the output field correlation (Ref Eq (2-47)) cannot, in general, be separated into a product of a spatial correlation and a temporal correlation, the output field due to a coherence separable source field is <u>not</u> coherence separable.

TABLE I

Special Forms of Output Spatial Correlation
Coherence Separable Source Fields

Type of Source	Emission Spectrum	Complex Degree of Coherence	Output Spatial Correlation $\Gamma_2(\bar{r}_2,\bar{r}_2')$
Monochromatic, Spatially Coherent (Ref 20:108)	$\delta(f)$	1	$(\frac{1}{\lambda_0 Z})^2 \int d\bar{r}_1\, u_1(\bar{r}_1)\exp[j\frac{k_0}{2Z}\lvert\bar{r}_2-\bar{r}_1\rvert^2] \int d\bar{r}_1'\, u_1^*(\bar{r}_1')\exp[-j\frac{k_0}{2Z}\lvert\bar{r}_2'-\bar{r}_1'\rvert^2]$
Monochromatic, Spatially Incoherent (Ref 14:510 and Eq (2-61))	$\delta(f)$	$\delta(\bar{r}_1-\bar{r}_1')$	$(\frac{1}{\lambda_0 Z})^2 \exp[j\psi_0] \int d\bar{r}_1\, I_1(\bar{r}_1)\exp[-j\frac{k_0}{Z}\,\bar{r}_1\cdot(\bar{r}_2-\bar{r}_2')]$
Broadband, Spatially Coherent (Ref Eq (2-56))	$S_w(f)$	1	$(\frac{1}{\lambda_0 Z})^2 \int d\bar{r}_1 \int d\bar{r}_1'\, u_1(\bar{r}_1)u_1^*(\bar{r}_1') \hat{R}_w[\frac{1}{2Z_c}(\lvert\bar{r}_2-\bar{r}_1\rvert^2-\lvert\bar{r}_2'-\bar{r}_1'\rvert^2)] \exp[j\frac{k_0}{2Z}(\lvert\bar{r}_2-\bar{r}_1\rvert^2-\lvert\bar{r}_2'-\bar{r}_1'\rvert^2)]$
Broadband, Spatially Incoherent (Ref Eq (2-57))	$S_w(f)$	$\delta(\bar{r}_1-\bar{r}_1')$	$(\frac{1}{\lambda_0 Z})^2 \exp[j\psi_0] \int d\bar{r}_1\, I_1(\bar{r}_1)\exp[-j\frac{k_0}{Z}\,\bar{r}_1\cdot(\bar{r}_2-\bar{r}_2')] \hat{R}_w[\frac{1}{2Z_c}(\lvert\bar{r}_2\rvert^2-\lvert\bar{r}_2'\rvert^2-\bar{r}_1\cdot(\bar{r}_2-\bar{r}_2'))]$

III. APPLICATION OF BROADBAND FIELD MODEL TO THE ANALYSIS OF A WHITE-LIGHT SHEARING INTERFEROMETER

A lateral shear AC interferometer has been used in the measurement of the phase-front of an optical wave. This chapter presents a description of this interferometer's operation for broadband optical fields with arbitrary spatial coherence based on the propagation models for broadband optical fields developed in Chapter II. The study of the shearing interferometer is intended to demonstrate the use of the broadband coherence model in the analysis of a broadband optical system. The fundamental limitations imposed on the wavefront measurement by the broadband nature of the optical field are sought. As such, the analysis ignores all diffraction effects due to finite aperture size and all lenses are assumed to be perfectly transmissive and aberration-free.

The first section presents a general discussion of the interferometer optics, summarizing results reported by Refs 7 and 10. The sections that follow present the analysis of the interferometer using the broadband coherence model. The phase which is measured by the interferometer is shown to be related to the phase of the complex part of the aperture field envelope. Results of this chapter show the effect of white-light optical fields on the interferometer's phase measurement. The median wavelength of white-light λ_0 is assumed to be 0.55 μm.

Description of Interferometer Optics

The lateral shear AC interferometer has been used to measure the local slope of an optical wavefront (Refs 7, 8, 9, and 10). As shown in Figure 4, the incoming wave is beamsplit into two similar channels, each consisting

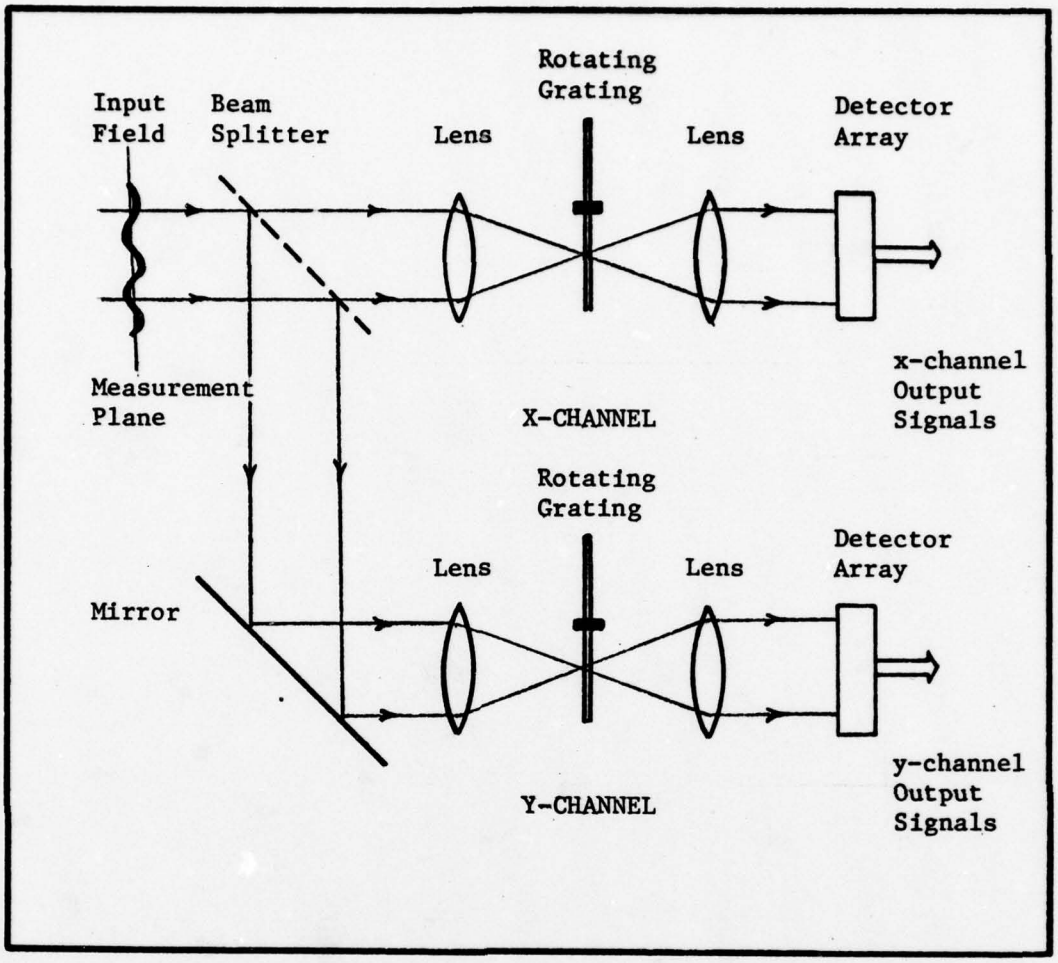

Figure 4. Two-Channel AC (Heterodyne) Shearing Interferometer

of a pair of lenses, a rotating radial grating, and a detector array. The purpose of each channel is to measure the wavefront slope along one of the two coordinate axes of the measurement plane. Output signals from the x- and y- channels can then be used to reconstruct a phase map of the two-dimensional wavefront sensed by the interferometer.

The optics in each channel are configured as in Figure 5. The two-dimensional optical field in the input aperture plane P_a is denoted

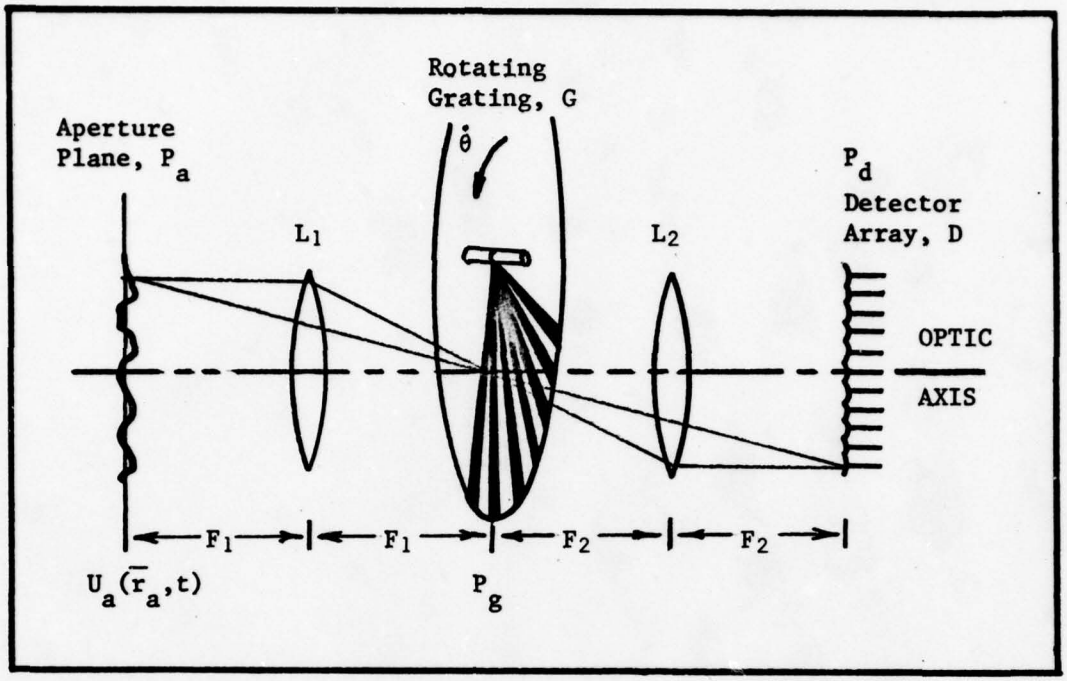

Figure 5. One-Channel Interferometer Optics

$U_a(\bar{r},t)$, where $\bar{r}_a = (x_a,y_a)$ are points in plane P_a . The input aperture of each channel coincides with the measurement plane shown in Figure 4, so that the interferometer measures the phase of $U_a(\bar{r}_a,t)$.

The input field is focused onto a rotating radial grating G in Plane P_g by a diffraction limited, chromatically compensated (apochromatic) lens L_1 having focal length F_1 . By diffraction limited and apochromatic it is meant that the lens will focus a plane wave located at P_a to a diffraction limited spot at plane P_g for all wavelengths. The field at the grating $U_g(\bar{r}_g,t)$ is chopped by the moving grating and focused onto a detector array at plane P_d by lens L_2 . Lens L_2 has focal length F_2 and is assumed to be apochromatic and diffraction limited.

The field chopped by the grating is diffracted, forming multiple images of the input field $U_a(\bar{r}_a,t)$ on the detector plane. Each diffracted image is shifted, or sheared, with respect to the next by an amount

$$s = \frac{\lambda F_2}{d} \qquad (3\text{-}1)$$

where s is the shear distance

F_2 is the focal length of lens L_2

d is the line spacing of grating (grating period)

λ is the wavelength of light

The direction of shear depends on the coordinate direction the rotating grading cuts the field in plane P_g.

The radial grating is a circular glass disc with alternating clear and opaque radial lines extending from near the center of the disc to its outer edge. If the grating has N opaque lines, the line spacing at a distance R from the center of the disc $d = 2\pi R/N$. Since the grating produces a square-wave transmittance at any radius it is also called a radial Ronchi grating. For the x-channel of the interferometer, the input field is focused onto the grating so that the Ronchi rulings move across the spot in the x-direction. The resulting diffraction causes the images in the detector plane to shear along the x-axis. In the y-channel, the radial lines cut the spot along the y-axis producing a y-shear in the detector plane. Figure 6 gives a representation of the lateral-sheared images of the input field for the x- and y-channels showing the zero, -1, and +1 diffracted orders. Each channel is constructed so that the focus point on the grating is variable and the shear distances in the x and y directions may be varied independently.

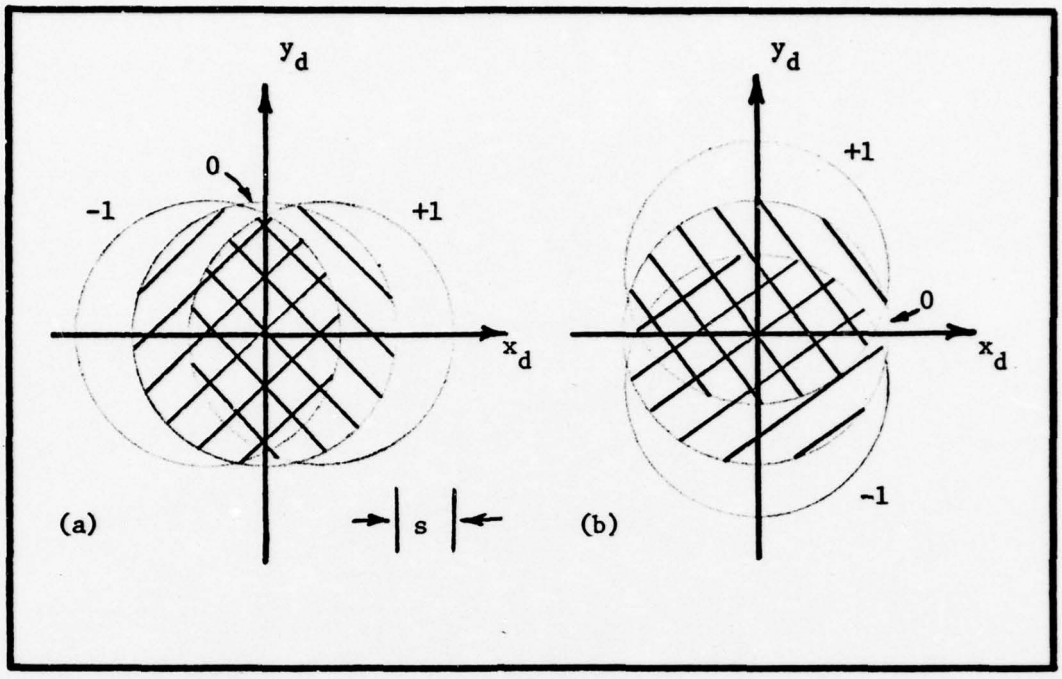

Figure 6. Representation of Lateral Sheared Images in Detector Plane for (a) x-shear and (b) y-shear Showing the +1, 0, and -1 Diffracted Orders.

As the gratings rotate, the intensity pattern at each point in the detector plane is modulated, producing an AC signal at the output of each detector. The fundamental modulation frequency f_s is given by

$$f_s = \frac{v_g}{d} = \frac{N\dot{\theta}}{2\pi} \tag{3-2}$$

where v_g is the linear speed of the radial grating at radius R in centimeters per second

d is the grating period at radius R in centimeters

N is the number of opaque lines in the grating

$\dot{\theta}$ is the angular speed of the grating in radians per second

As it is shown later, the fundamental frequency corresponds to the interference of the zero and +1, with the zero and -1 diffracted orders in the

shaded region of the detector plane shown in Figure 6. If the square-wave Ronchi grating is used, no other combination of diffraction orders produces an interference pattern modulated at f_s. It is to be shown how the detector plane interference pattern modulated at f_s relates to the phase of a broadband input field $U_a(\bar{r}_a,t)$.

Calculation of Detector Field

The propagation geometry for the x-channel of the lateral shear AC interferometer is shown in Figure 7. The broadband field $U_a(\bar{r}_a,t)$ located in the input aperture (measurement plane) P_a of the interferometer can be expanded into temporal modes:

$$U_a(\bar{r}_a,t) = \sum_n u_{an}(\bar{r}_a) w_n e^{+j2\pi \frac{n}{T} t}$$

$$\text{for } -\frac{T}{2} < t < \frac{T}{2} \qquad (3\text{-}3)$$

where $u_{an}(\bar{r}_a)$ is the spatial part of the aperture field and the sum over temporal modes n converges in the mean-square. Note that the aperture field is decomposed such that the spatial variations of the field depend on wavelength. As written in Eq (3-3) the aperture field is not coherence separable. If for instance, the aperture field is due to a field which had propagated some distance to the aperture plane, the output field consists of a sum of individually propagated temporal modes (Ref (2-42)), and the spatial part of each mode is given by Eq (2-36). To simplify the analysis later in this chapter, it will be assumed at a later point that the input field is coherence separable, and as such, the spatial variations of the aperture plane are the same for all temporal modes. This assumption will allow the calculation of the phase of an aperture

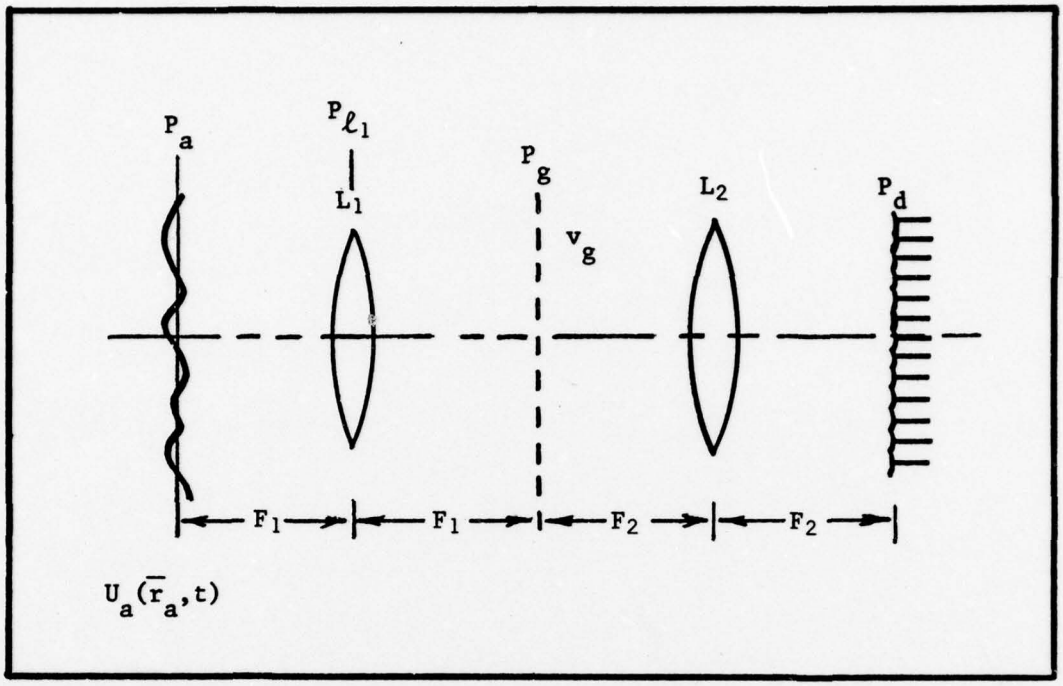

Figure 7. Propagation Geometry for X-Channel Interferometer Optics

field whose spatial content is independent of wavelength. If $U_a(\bar{r}_a,t)$ were coherence separable, Eq (3-3) would be written

$$U_a(\bar{r}_a,t) = u_a(\bar{r}_a) \sum_n w_n e^{+j2\pi \frac{n}{T} t}$$

for $-\frac{T}{2} < t < \frac{T}{2}$ (3-4)

where $u_a(\bar{r}_a)$ is the wavelength-independent spatial part of the aperture field. The discussion of phase measurement for a temporally broadband field which is not coherence separable is presented in Chapter IV where the interferometer is applied to the situation where the aperture field has a phase which has been distorted by atmospheric turbulence.

Using the free-space propagation model for temporally broadband fields expressed in Eq (2-38), the n^{th} temporal mode of the optical field just prior to lens L_1 can be written

$$U_{\ell_{1n}}(\bar{r}_{\ell_1},t) = \frac{e^{jk_nF_1}}{j\lambda_nF_1}\int d\bar{r}_a\, U_{an}(\bar{r}_a,t)\exp[j\frac{k_n}{2F_1}\,|r_{\ell_1}-r_a|^2]$$

for $-\frac{T}{2} < t < \frac{T}{2}$ (3-5)

where

$$U_{an}(\bar{r}_a,t) = u_{an}(\bar{r}_a)w_n e^{+j2\pi\frac{n}{T}t} \tag{3-6}$$

represents the n^{th} temporal mode of the aperture field, and $U_{\ell_{1n}}(\bar{r}_{\ell_1},t)$ is the n^{th} mode of the field at lens plane P_{ℓ_1} just prior to thin lens L_1.

Apochromatic Lens Model. Following Goodman (Ref 20:81), a lens performs a quadratic phase transformation on the incident field. For a white-light incident field $U_{\ell_1}(\bar{r}_{\ell_1},t)$ an apochromatic lens performs a quadratic phase transformation on the broadband field in the following way:

$$U'_{\ell_{1n}}(\bar{r}_{\ell_1},t) = U_{\ell_{1n}}(\bar{r}_{\ell_1},t)\exp[-j\frac{\pi}{\lambda_nF_1}\,(x_\ell^2+y_\ell^2)]$$

for $-\frac{T}{2} < t < \frac{T}{2}$ (3-7)

where $U'_{\ell_{1n}}(\bar{r}_{\ell_1},t)$ is the n^{th} temporal mode of the field just to the right of lens L_1. The n^{th} field mode just prior to the grating in plane P_g given by the $U_{gn}(\bar{r}_g,t)$, is the result of propagating $U'_{\ell_{1n}}(\bar{r}_{\ell_1},t)$ a distance F_1 to the focal plane of the lens:

$$U_{gn}(\bar{r}_g,t) = \frac{e^{jk_nF_1}}{j\lambda_nF_1}\int d\bar{r}_{\ell_1}U_{\ell_1}(\bar{r}_{\ell_1},t)\exp[-j\frac{\pi}{\lambda_nF_1}\,|\bar{r}_{\ell_1}|^2]$$

$$\exp[j\frac{k_n}{2F_1}\,|\bar{r}_g-\bar{r}_{\ell_1}|^2] \tag{3-8}$$

$$= \frac{e^{jk_n2F_1}}{j\lambda_nF_1}\exp[j\frac{k_n}{2F_1}\,|\bar{r}_g|^2]$$

$$\int d\bar{r}_{\ell_1}U_{\ell_{1n}}(r_{\ell_1},t)\exp[-j\frac{2\pi}{\lambda_nF_1}\,r_g\cdot r_{\ell_1}] \tag{3-9}$$

By substituting Eq (3-5) into (3-9) and solving the integral over $\bar{r}_{\ell_1}$, assuming the lens is of infinite extent, yields

$$U_{gn}(\bar{r}_g,t) = \frac{e^{jk_n 2F_1}}{j\lambda_n F_1} \int d\bar{r}_a \; U_{an}(\bar{r}_a,t)\exp[-j\frac{k_n}{F_1}\,\bar{r}_g\cdot\bar{r}_a]$$

for $-\frac{T}{2} < t < \frac{T}{2}$. (3-10)

Note that for each temporal mode, the spatial part of the grating field is an exact two-dimensional Fourier transform of the input spatial field:

$$U_{gn}(\bar{r}_g) = \frac{e^{jk_n 2F_1}}{j\lambda_n F_1} \int d\bar{r}_a \; u_{an}(\bar{r}_a)\exp[-j\,2\pi(\frac{\bar{r}_g}{\lambda_n F_1})\cdot\bar{r}_a] \qquad (3\text{-}11)$$

$$= \frac{1}{j\lambda_n F_1}\; \exp[j\; k_n 2F_1]\; F_{x_a y_a}\{u_{an}(\bar{r}_a)\} \qquad (3\text{-}12)$$

where $u_{an}(\bar{r}_a)$ and $u_{gn}(\bar{r}_g)$ are the time-independent parts of the aperture and grating fields, respectively; $F_{x_a y_a}\{\cdot\}$ denotes a two-dimensional Fourier transform with respect to variables x_a and y_a; and the transform is evaluated at spatial frequencies $f_x = x_g/(\lambda_n F_1)$ and $f_y = y_g/(\lambda_n F_1)$. The broadband field at the grating is, therefore, the superposition of Fourier transforms defined for each temporal mode. This result may be considered a white-light extension to the Fourier transforming properties of F-F optical systems (Ref 20:86-87) where the input field can be decomposed as in Eq (3-3). If the lens L_1 were not apochromatic as defined, the transform results (3-11) and (3-12) would not hold for the field at grating plane P_g .

Rotating Grating Model. Since the radial grating is assumed to be periodic in x_g for the x-channel of the interferometer, its transmission function can be expanded in a Fourier series. The n^{th} mode of the chopped field just beyond the rotating grating $U'_{gn}(\bar{r}_g,t)$ can then be written

$$U'_{gn}(\bar{r}_g,t) = U_{gn}(\bar{r}_g,t) \sum_m G_m \exp[j2\pi \frac{m}{d}(x_g - v_g t)] \qquad (3\text{-}13)$$

where $U_{gn}(\bar{r}_g,t)$ is the n^{th} temporal mode of the optical field incident on the rotating radial grating given in Eq (3-12)

$$G_m = \frac{1}{m\pi} e^{j\frac{\pi}{2}m} \sin(\frac{m\pi}{2}) \qquad (3\text{-}14)$$

is the Ronchi (square-wave) grating coefficient of the m^{th} diffracted order for all integers $m \neq 0$, where $G_0 = \frac{1}{2}$

$$d = \frac{2\pi R}{N} \qquad (3\text{-}15)$$

is the grating period of an N line radial grating at distance R from the center of the disc, and

$$v_g = R\dot{\theta} \qquad (3\text{-}16)$$

is the speed of the grating in the x_g-direction, $\dot{\theta}$ is the angular speed of the grating in radians per second.

Note that the phase of the grating coefficients G_m given in Eq (3-14) indicates an asymmetrical positioning of the grating with respect to the x_g-axis at $t = 0$. Specifically, a time reference may be defined so that $t = 0$ whenever the position of the grating allows its Fourier coefficients to be given by Eq (3-14). This time reference is necessary for the extraction of the phase measurement from the interferometer output signal.

Detector Plane Field. Using the broadband propagation result for apochromatic lens F-F optical systems similar to the one expressed in Eq (3-10), the n^{th} optical field mode at the detector plane $U_{dn}(\bar{r}_d,t)$ due to the broadband field $U_g'(\bar{r}_g,t)$ is

$$U_{dn}(\bar{r}_d,t) = \frac{1}{j\lambda_n F_2} \exp[jk_n 2F_2] \int d\bar{r}_g \; U\acute{g}_n(\bar{r}_g,t)\exp[-j\frac{k_n}{F_2}\,\bar{r}_d\cdot\bar{r}_g]$$

for $-\frac{T}{2} < t < \frac{T}{2}$. (3-17)

Combining Eqs (3-10), (3-13), and (3-17) and carrying out the two-dimensional integral over the grating plane P_g yields an expression for the n^{th} temporal mode of the detector field in terms of the aperture field:

$$U_{dn}(\bar{r}_d,t) = \sum_m M\, G_m \exp[j2k_n(F_1+F_2)]\exp[-j2\pi m f_s t] \; U_{an}[M(x_d - ms_0), My_d, t]$$

for $-\frac{T}{2} < t < \frac{T}{2}$ (3-18)

where

$$M = \frac{-F_1}{F_2} \tag{3-19}$$

is the magnification of the two lens, double F-F optical system, f_s is the fundamental modulation frequency of the detector field given previously in Eq (3-2)

$$s_n = \frac{s_0}{\xi(n)} = \frac{\lambda_0 F_2}{d}\;\xi^{-1}(n) \tag{3-20}$$

is the shear distance for the n^{th} temporal mode, and s_0 is the shear distance for the median wavelength λ_0, measured in the detector plane. The expression for $U_{an}(\bar{r}_a,t)$ is given in Eq (3-6).

The detector field of the x-channel for each temporal mode n and each diffracted order m is, therefore, a scaled and shifted image of the input field mode $U_{an}(\bar{r}_a,t)$ modulated at frequency mf_s. Note that the modulation frequency and scaling of the field are independent of wavelength. The location (or relative shear) of each diffracted order, however, depends on temporal mode--and therefore, on wavelength. The amount of x-shear for each diffracted order m is, from Eq (3-20)

$$ms_n = m\frac{\lambda_n F_2}{d} \tag{3-21}$$

The effect of this wavelength dependence on the interferometer's phase measurement for aperture fields with various states of spatial coherence is shown in the last two sections of this chapter.

Following the propagation model for broadband fields (2-40) the broadband detector field $U_a(\bar{r}_d,t)$ is written as the sum of all the individually propagated modes:

$$U_d(\bar{r}_d,t) = \sum_n U_{dn}(\bar{r}_d,t) \tag{3-22}$$

Analysis of Detector Plane Intensity Pattern

The light-intensity on the detector plane $I_d(\bar{r}_d,t)$ due to the broadband field is given by

$$I_d(\bar{r}_d,t) \triangleq \left\langle U_d(\bar{r}_d,t)U_d^*(\bar{r}_d,t)\right\rangle \tag{3-23}$$

$$= \sum_n \sum_{n'} \left\langle U_{dn}(\bar{r}_d,t)U_{dn'}^*(\bar{r}_d,t)\right\rangle \tag{3-24}$$

where n and n' range over all significant temporal modes of the broadband process $w(t)$. Note that each field mode $U_{dn}(\bar{r}_d,t)$ given in Eq (3-18) is the sum of all the field orders m diffracted by the rotating grating. The interference of all diffracted temporal modes must therefore be written as a double sum over m. The detector plane intensity may also be written

$$I_d(\bar{r}_d,t) = \sum_m \sum_{m'} \sum_n \sum_{n'} \left\langle U_{dnm}(\bar{r}_d,t) U^*_{dn'm'}(\bar{r}_d,t) \right\rangle \qquad (3\text{-}25)$$

where

$$U_{dnm}(\bar{r}_d,t) = M\, G_m \exp[j2k_n(F_1+F_2)] \cdot \exp[-j2\pi m f_s t] \cdot U_{an}(M(\bar{r}_d - ms_n),t) \qquad (3\text{-}26)$$

is the m^{th} diffracted order of the n^{th} temporal mode of the x-sheared detector field. In (3-25) the indices m and m' range over all integer values for which the grating coefficients G_m and $G_{m'}$ have significant value. In Eq (3-26) the vector form of the shear is used so that $\bar{s}_n = (s_n,0)$ indicates an x-shear of s_n for each temporal mode n, and no shear in the y-direction in the detector plane.

The ensemble field intensity can be greatly simplified. Note that in the intensity calculation, the modal expansion of the broadband process $w(t)$ has reduced an ensemble average over the sample functions to an expected value over a sum of random variables w_n and $w_{n'}$. Using the fact that the modal expansion coefficients $\{w_n\}$ are uncorrelated, as expressed in Eq (2-24), Eq (3-25) may be written:

$$I_d(\bar{r}_d,t) = \sum_m \sum_{m'} M^2 G_m G_{m'}^* \exp[-j2\pi(m-m')f_s t]$$

$$\Gamma_a(M(\bar{r}_d - ms_n), M(\bar{r}_d - m's_n)) \tag{3-27}$$

where
$$\Gamma_a(\bar{r}_a,\bar{r}_a') = \left\langle U_a(\bar{r}_a,t)U_a^*(\bar{r}_a',t)\right\rangle \tag{3-28}$$

$$= \frac{1}{T}\sum_n S_w(\frac{n}{T})\left\langle u_{an}(\bar{r}_a)u_{an}^*(\bar{r}_a')\right\rangle \tag{3-29}$$

is the spatial correlation of the broadband aperture field $U_a(\bar{r}_a,t)$ evaluated at points $\bar{r}_a$ and $\bar{r}_a'$.

From Eq (3-27) it can be seen that the intensity pattern modulated in time at frequency f_s results from the coherent addition of two diffracted orders m and m' such that $|m-m'| = 1$. Using the Ronchi grating coefficients $\{G_m\}$ defined in Eq (3-14), the intensity pattern modulated at f_s is calculated:

$$i_d(\bar{r}_d,t) = \frac{M^2}{\pi}\mathrm{Re}\{\exp[-j(2\pi f_s t - \frac{\pi}{2})]\Gamma_a(M(\bar{r}_d - \bar{s}_n), M\bar{r}_d)\}$$

$$+ \frac{M^2}{\pi}\mathrm{Re}\{\exp[+j(2\pi f_s t - \frac{\pi}{2})]\Gamma_a(M(\bar{r}_d + \bar{s}_n), M\bar{r}_d)\}$$

$$\text{for } -\frac{T}{2} < t < \frac{T}{2} \tag{3-30}$$

where $i_d(\bar{r}_d,t)$ is the intensity pattern at the detector plane at frequency f_s for x-shear, and the double sum over diffraction orders is calculated such that $|m-m'| = 1$ for all terms in the summation. The intensity pattern $i_d(\bar{r}_d,t)$ at each point (x_d,y_d) in the detector plane is defined to be the x-channel output signal of the AC interferometer.

Each detected signal mode n is composed of two similar terms modulated at frequency f_s. The first term is the result of the coherent addition of the $m = +1$ and $m = 0$ field orders diffracted by the rotating grating. This term will be called the "positive-shear" term because it contains the correlation of the +1 diffracted order, sheared by distance $+s_n$ in the detector plane, with the undiffracted field order. The second term results from the interference of the $m = -1$ and $m = 0$ diffracted orders and is called the "negative-shear" term.

Since the spatial part of the aperture field mode is independent of time, no additional frequency modulation is introduced into the detector signal.

Phase Measurement for Coherence Separable Aperture Fields

In this section the interferometer phase measurement is derived for aperture fields which may be assumed to be coherence separable. Such fields which can be characterized by an expansion over its temporal modes may be written as in Eq (3-4). Following Eq (3-28), the spatial correlation of the coherence separable aperture field may be written

$$\Gamma_a(\bar{r}_a,\bar{r}_a') = \frac{1}{T}\sum_n S_w(\tfrac{n}{T}) \left\langle u_a(\bar{r}_a)u_a^*(\bar{r}_a') \right\rangle \tag{3-31}$$

$$= \frac{1}{T}\sum_n S_w(\tfrac{n}{T})\, R_a(\bar{r}_a,\bar{r}_a') \tag{3-32}$$

where $R_a(\bar{r}_a,\bar{r}_a')$ is the correlation of the spatial part of the aperture field defined in Eq (2-5). Allowing the spatial correlation $R_a(\bar{r}_a,\bar{r}_a')$ to be written in terms of its complex degree of coherence (Ref Eq (2-53))

$$R_a(\bar{r}_a,\bar{r}_a') = \tilde{\mu}_a(\bar{r}_a,\bar{r}_a')u_a(\bar{r}_a)u_a^*(\bar{r}_a') \tag{3-33}$$

where $\tilde{\mu}_a(\bar{r}_a,\bar{r}_a')$ is the complex degree of coherence of the aperture field, the detector signal for x-shear may be written

$$i_d(\bar{r}_d,t) = \frac{M^2}{\pi}\ \mathrm{Re}\{\exp[-j(2\pi f_s t - \tfrac{\pi}{2})]\ u_a^*(M\bar{r}_d)$$

$$\frac{1}{T}\ \sum_n S_w(\tfrac{n}{T})\tilde{\mu}_a(M(\bar{r}_d-s_n),M\bar{r}_d)u_a(M(\bar{r}_d-\bar{s}_n))\}$$

$$+\ \frac{M^2}{\pi}\ \mathrm{Re}\{\exp[+j(2\pi f_s t - \tfrac{\pi}{2})]u_a^*(M\bar{r}_d)$$

$$\frac{1}{T}\sum_n S_w(\tfrac{n}{T})\tilde{\mu}_a(M(\bar{r}_d+\bar{s}_n),M\bar{r}_d)u_a(M(\bar{r}_d+\bar{s}_n),M\bar{r}_d)\}$$

for $-\frac{T}{2} < t < \frac{T}{2}$ (3-34)

where all the mode-dependent terms have been grouped together.

Let

$$\hat{u}_a(M(\bar{r}_d-\bar{s}_0)) = \frac{1}{T}\sum_n S_w(\tfrac{n}{T})\tilde{\mu}_a(M(\bar{r}_d-\bar{s}_n),M\bar{r}_d)$$

$$\cdot\, u_a(M(\bar{r}_d-\bar{s}_n)) \quad (3-35)$$

and

$$\hat{u}_a(M(\bar{r}_d+\bar{s}_0)) = \frac{1}{T}\sum_n S_w(\tfrac{n}{T})\tilde{\mu}_a(M(\bar{r}_d+\bar{s}_n),M\bar{r}_d)$$

$$\cdot\, u_a(M(\bar{r}_d+\bar{s}_n)) \quad (3-36)$$

Furthermore, let all spatial fields be written in polar form:

$$u_a(M\bar{r}_d) = A(M\bar{r}_d)\exp[j\phi(M\bar{r}_d)] \tag{3-37}$$

$$\hat{u}_a(M(\bar{r}_d-\bar{s}_0)) = \hat{A}(M(\bar{r}_d-\bar{s}_0))\exp[j\hat{\phi}(M(\bar{r}_d-\bar{s}_0))] \tag{3-38}$$

and

$$\hat{u}_a(M(\bar{r}_d+\bar{s}_0)) = \hat{A}(M(\bar{r}_d+\bar{s}_0))\exp[j\hat{\phi}(M(\bar{r}_d+\bar{s}_0))] \tag{3-39}$$

In the next section it will be shown that for white-light coherence separable aperture field envelopes, the lateral shear AC interferometer causes the $m = +1$ and $m = -1$ diffracted spatial field orders to be spatially low-pass filtered. The "hats" over the amplitude and phase of the diffracted orders indicate that they represent the amplitude and phase of the spatially filtered field. The nature of this spatial filtering is generally discussed for coherence separable broadband fields in the next section, and discussed specifically for broadband, spatially incoherent source fields in Chapter IV. Note that the spatially filtered, diffracted field orders are defined with respect to the shear distance s_0 for the median wavelength of white-light. Whereas the performance of the interferometer is analyzed with respect to s_0, it may be used as a design parameter for a physically realizable interferometer.

Note that the $m = 0$, or undiffracted order, is not filtered. The spatial filtering of the diffracted orders can be thought of as being

caused by differential path length effects associated with the diffraction of broadband light by the interferometer's rotating grating. If the field is not diffracted, there are no differential paths and no spatial filtering is introduced.

Using the expressions given above for the zero (3-37), m = +1, (3-38), and m = -1 (3-39) diffracted field orders, Eq (3-34) may be rewritten

$$i_d(\bar{r}_d,t) = \frac{M^2}{\pi} A(M\bar{r}_d)\hat{A}(M(\bar{r}_d-\bar{s}_0))\mathrm{Re}\{\exp[-j(2\pi f_s t - \tfrac{\pi}{2})]$$

$$\exp[j\hat{\phi}(M(\bar{r}_d-\bar{s}_0))-j\phi(M\bar{r}_d)]\}$$

$$+ \frac{M^2}{\pi} A(M\bar{r}_d)\hat{A}(M(\bar{r}_d+\bar{s}_0)\mathrm{Re}\{\exp[+j(2\pi f_s t - \tfrac{\pi}{2})]$$

$$\exp[j\hat{\phi}(M(\bar{r}_d+\bar{s}_0))-\phi(M\bar{r}_d)]\}$$

for $-\frac{T}{2} < t < \frac{T}{2}$. (3-40)

If the amplitudes of the spatially filtered orders are assumed to be equal over the distance of the shear for each point in the detector plane

$$\hat{A}(M\bar{r}_d) \simeq \hat{A}(M(\bar{r}_d-\bar{s}_0)) \quad (3\text{-}41)$$

$$\simeq \hat{A}(M(\bar{r}_d+\bar{s}_0)) \quad (3\text{-}42)$$

where $\hat{A}(x_a,y_a)$ is the amplitude of both sheared field orders, the positive and negative-shear terms may be combined and Eq (3-40) may be simplified:

$$i_d(\bar{r}_d,t) = \frac{2M^2}{\pi} A(M\bar{r}_d)\hat{A}(M\bar{r}_d)$$

$$\cos\left[\frac{1}{2}(\hat{\phi}_+ + \hat{\phi}_-) - \phi\right]$$

$$\sin\left[2\pi f_s t + \frac{1}{2}(\hat{\phi}_- - \hat{\phi}_+)\right]$$

for $-\frac{T}{2} < t < \frac{T}{2}$ (3-43)

where $\phi = (M\bar{r}_d)$ (3-44)

$$\hat{\phi}_+ = \hat{\phi}(M(\bar{r}_d - \bar{s}_0)) \quad (3-45)$$

$$\hat{\phi}_- = \hat{\phi}(M(\bar{r}_d + \bar{s}_0)) \quad (3-46)$$

Eq (3-43) represents the interferometer output signal for x-shear in terms of the amplitudes and phases of the sheared (and filtered) aperture field orders. The aperture phase measurement made by the interferometer output signal is

$$\Delta\hat{\phi} = \hat{\phi}_- - \hat{\phi}_+ \quad (3-47)$$

It is shown in later sections how the measured phase $\Delta\hat{\phi}$ relates to the spatial part of the broadband aperture field for special cases of aperture field coherence.

If the amplitudes of the spatially filtered orders are <u>not</u> equal over the distance of shear as assumed in Eqs (3-41) and (3-42), the resulting detector signal is rewritten

$$i_d(\bar{r}_d,t) = \frac{M^2}{\pi} A(M\bar{r}_d)$$

$$\{\hat{A}(M(\bar{r}_d-\bar{s}_0)) \sin[2\pi f_s t-\hat{\phi}(M(\bar{r}_d-\bar{s}_0))+\phi(M\bar{r}_d)]$$

$$+ \hat{A}(M(\bar{r}_d+s_0)) \sin[2\pi f_s t$$

$$+ \hat{\phi}(M(\bar{r}_d+\bar{s}_0))-\phi(M\bar{r}_d)]\} \qquad (3\text{-}48)$$

Eq (3-48) can be interpreted as a sum of two phasors with phases

$$\phi_P = -\hat{\phi}(M(\bar{r}_d-\bar{s}_0)) + \phi(M\bar{r}_d) \qquad (3\text{-}49)$$

due to the positive-shear term, and

$$\phi_N = +\hat{\phi}(M(\bar{r}_d+\bar{s}_0)) - \phi(M\bar{r}_d) \qquad (3\text{-}50)$$

due to the negative shear term as indicated in Figure 8. The resulting amplitude $\hat{A}_R$ and phase $\hat{\phi}_R$ of the detector signal is the sum of the positive- and negative-shear phasor terms as indicated in Figure 8. Henceforth, it will be assumed that the amplitudes of the spatially filtered diffracted fields are nearly equal so that Eq (3-43) adequately represents the interferometer output signal for x-shear. It is shown in Chapter IV that for the case of distant sources, this assumption is, indeed, valid.

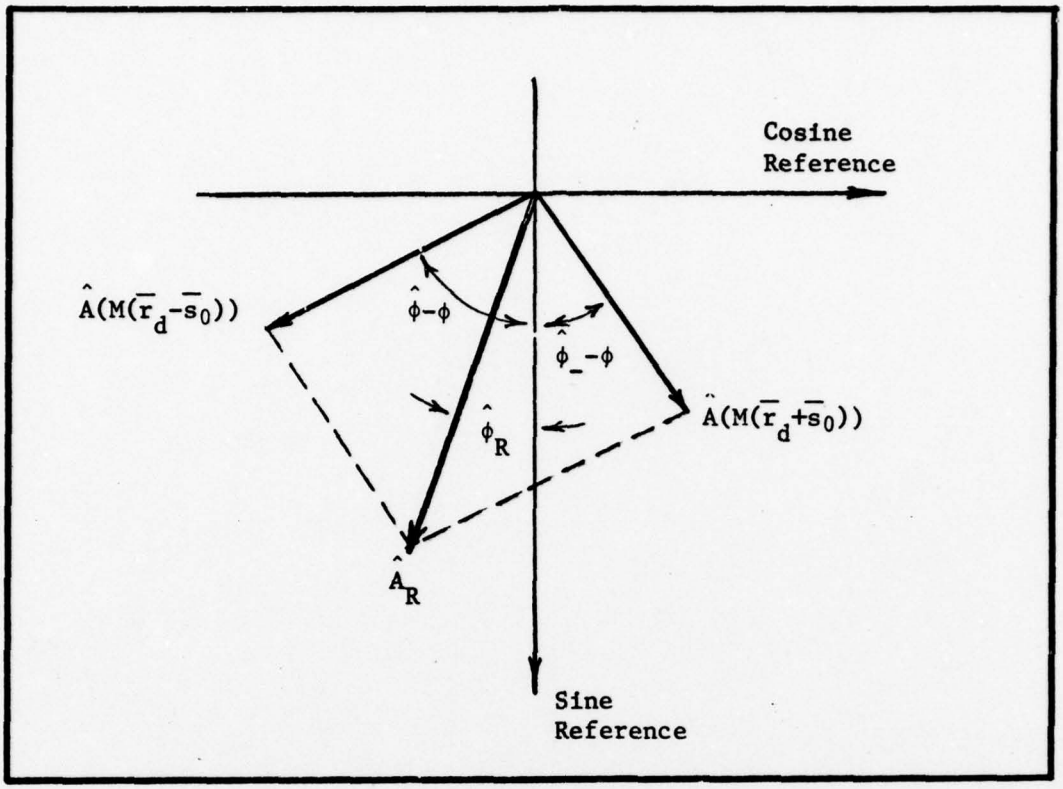

Figure 8. Phasor Addition of Positive and Negative Shear Terms

The next section shows that the lateral shear AC interferometer causes the diffracted orders of the coherence separable white-light aperture field to be filtered, giving rise to a filtered phase $\Delta\hat{\phi}$ which is ultimately measured.

Spatial Filtering Effects of White-Light Interferometer

Consider the following term defined in Eq (3-35) representing the spatial part of the $m = +1$ diffracted order in the detector plane:

$$\hat{u}_a(M(\bar{r}_d-\bar{s}_0)) = \frac{1}{T}\sum_n S_w(\tfrac{n}{T})\tilde{u}_a(M(\bar{r}_d-\bar{s}_n),M\bar{r}_d)u_a(M(\bar{r}_d-\bar{s}_n)) \qquad (3\text{-}51)$$

If $\tilde{\mu}_a(\bar{r}_a,\bar{r}_a')$ is homogeneous across the aperture of the interferometer, the complex degree of coherence of the aperture field may be written

$$\tilde{\mu}_a(\bar{r}_a,\bar{r}_a') = \tilde{\mu}_a(\bar{r}_a - \bar{r}_a') \tag{3-52}$$

Assuming $\tilde{\mu}_a$ homogeneous allows (3-51) to be written

$$\hat{u}_a(M(\bar{r}_d-\bar{s}_0)) = \frac{1}{T}\sum_n S_w(\frac{n}{T})\tilde{\mu}_a(M\bar{s}_n)u_a(M(\bar{r}_d-\bar{s}_n)) \tag{3-53}$$

Note that $\tilde{\mu}_a$ is evaluated for a separation of $M\bar{s}_n$ in the x-direction and no separation in the y-direction. Taking the spatial Fourier transform of Eq (3-53) with respect to the aperture plane coordinates yields

$$F_{x_a y_a}\{\hat{u}_a(M(\bar{r}_d-\bar{s}_0))\}$$

$$= \frac{1}{T}\sum_n S_w(\frac{n}{T})\mu_a(M\bar{s}_n)\ V_a(f_x,f_y)e^{-j2\pi f_x M s_0 \xi^{-1}(n)} \tag{3-54}$$

where

$$V_a(f_x,f_y) = F_{x_a y_a}\{u_a(x_a,y_a)\} \tag{3-55}$$

Using the binomial expansion for $\xi^{-1}(n)$ and approximating the infinite sum by the first two terms

$$\xi^{-1}(n) = (1-\frac{n}{f_0 T})^{-1} \simeq 1 + \frac{n}{f_0 T} \tag{3-56}$$

which is a good approximation for $\frac{n}{f_0 T} << 1$, allows (3-54) to be written in the following form:

$$F_{x_a y_a}\{\hat{u}_a(M(\bar{r}_d - \bar{s}_0))\} = V_a(f_x, f_y)\exp[-j2\pi f_x M s_0]$$

$$\frac{1}{T}\sum_n \tilde{\mu}_a\left(Ms_0\left(1+\frac{n}{f_0 T}\right)\right) S_w\left(\frac{n}{T}\right)$$

$$\exp\left[-j2\pi \frac{f_x M s_0}{f_0}\left(\frac{n}{T}\right)\right] \qquad (3\text{-}57)$$

The approximation in (3-56) assumes that although the power spectrum $S_w(f)$ is broad, its effective bandwidth B is still sufficiently small that the higher order terms of $\xi^{-1}(n)$ in the exponential of Eq (3-54) can be neglected. The maximum index n in the sum (3-57) is limited by the effective bandwidth B so that $\text{Max}(n) \simeq \pm BT$. Assuming that the power spectrum is still broadband enough that the sum over n may be approximated by an integral over v

$$F_{x_a y_a}\{\hat{u}_a(M(\bar{r}_d - \bar{s}_0))\} = V_a(f_x, f_y)\exp[-j2\pi f_x M s_0]$$

$$\int dv\ \tilde{\mu}_a\left(Ms_0\left(1+\frac{v}{f_0}\right)\right) S_w(v)$$

$$\exp\left[-j2\pi\left(\frac{f_x M s_0}{f_0}\right) v\right]$$

(3-58)

To first order then, Eq (3-58) expresses the spatial filtering effect of the AC shearing interferometer on the $m = +1$ diffracted field order, when the source field can be assumed to be coherence separable. Although Eq (3-58) indicates a doubly-infinite range of integration, the range of

v for which the integral has significant value is limited to the spectral bandwidth of $S_w(v)$ --which is nominally $-B < v < B$. Define

$$H_+(\zeta) = \int dv \tilde{u}_a(Ms_0(1 - \frac{v}{f_0}))\, S_w(v) \exp[-j2\pi\zeta v] \qquad (3\text{-}59)$$

where

$$\zeta = \frac{f_x Ms_0}{f_0} \qquad (3\text{-}60)$$

to be the spatial filter introduced by the interferometer's diffraction grating on the $m = +1$ field order. Note that there is no spatial filtering for spatial frequencies associated with the y-direction since no y-shear was introduced in the x-channel. The corresponding filter for the $m = +1$ order in the y-channel, therefore, does not affect the x-direction spatial frequencies.

The same analysis, when applied to the $m = -1$ diffracted order, yields

$$F_{x_a y_a}\{\hat{u}_a(M(\bar{r}_d + \bar{s}_0))\}$$

$$= V_a(f_x, f_y) \exp[+j2\pi f_x Ms_0] H_-(\zeta) \qquad (3\text{-}61)$$

where

$$H_-(\zeta) = \int dv\ \tilde{u}_a(Ms_0(1 + \frac{v}{f_0}))\, S_w(v) \exp[+j2\pi\zeta v] \qquad (3\text{-}62)$$

is the spatial filtering introduced into the $m = -1$ diffracted field order.

The form of spatial filtering functions H_+ and H_- is seen to depend on three effects: (1) the complex degree of coherence of the aperture field $\tilde{\mu}_a(\bar{r}_a - \bar{r}_a')$, (2) the power spectrum of the wide-band temporal process $S_w(f)$, and (3) the shear distance s_0 for the median light wavelength, defined by

$$s_0 = \frac{\lambda_0 F_2}{d} \tag{3-63}$$

The shear distance is a design parameter which may be chosen to fit a specific set of operating conditions. Since the coherence properties of broadband light are relatively insensitive to the precise functional form of the temporal process power spectrum, the ultimate forms of the spatial filtering functions are also relatively insensitive to the precise form of the broadband power spectrum $S_w(f)$. The dependence of the filtering effect on the specific coherence properties of the aperture field is, however, significant. In the next two sections, the effect of aperture field coherence, given a particular temporal power spectrum, are considered for special cases of the field's degree of coherence $\tilde{\mu}_a(\bar{r}_a, \bar{r}_a')$. The filtering effects of a specific form of $\tilde{\mu}_a(\bar{r}_a, \bar{r}_a')$ are considered in Chapter VI with the application of the shearing interferometer as a wavefront sensor in a phase-compensated imaging system.

Filtering Effects for Spatially Coherent Aperture Fields

For an aperture field which is spatially coherent, the complex degree of coherence is equal to unity for all points of interest in the aperture plane (Ref Eq (2-34)). Following Eq (3-59) the spatial filter H_+ may then be written

$$H_+(\zeta) = \int dv\ S_w(v)\exp[-j2\pi\zeta v] \tag{3-64}$$

$$= F_v\{S_w(v)\} \tag{3-65}$$

$$= R_w(\zeta) = R_w\left(\frac{f_x Ms_0}{f_0}\right) \tag{3-66}$$

where $F_v\{\cdot\}$ denotes the Fourier transform with respect to variable v, and the transform is evaluated at $\frac{f_x Ms_0}{f_0}$, and $R_w(\cdot)$ is the correlation of the broadband time process $w(t)$ defined in Eq (2-9). Note that since the correlation functions considered here are stationary and even

$$F_v\{S_w(v)\} = F_v^{-1}\{S_w(v)\} = R_w(\zeta) \tag{3-67}$$

Applying the same analysis to Eq (3-63) shows that the spatial filtering introduced into the -1 diffracted field order has the same form:

$$H_-(\zeta) = R_w(\zeta) \tag{3-68}$$

$$= H_+(\zeta) = H(\zeta) \tag{3-69}$$

As discussed in Chapter II (Ref Eq (2-73)), the correlation function $R_w(\tau)$ will drop off with increasing argument so as to limit the high spatial frequency content of $V_a(f_x,f_y)$ in Eq (3-58). Therefore, for white-light, spatially coherent aperture fields, the AC shearing interferometer causes the sheared orders of the broadband detector field to be spatially low-pass filtered. The form of this filtering has been

shown to be, to first order, the correlation function of the broadband temporal process $w(t)$ evaluated at $\tau = \frac{f_x Ms_0}{f_0}$.

As an example calculation, consider the bandlimited power spectrum $S_b(f)$ and its correlation function $R_b(\tau) = F_f^{-1}\{S_b(f)\}$. The correlation function resembles a $\sin(x)/x$ function with the first zero-crossing at

$$\zeta = \frac{f_x Ms_0}{f_0} = \frac{1}{2B} = \tau_b \tag{3-70}$$

where B is the bandwidth of $S_b(f)$, τ_b is the argument of $R_b(\tau)$ for which $R_b(\tau) \simeq 0$, and the argument of the spatial filtering function $H(\zeta)$ has been equated with that of the correlation function $R_b(\tau)$. Define the effective spatial bandwidth of the filtering function $H(\frac{f_x Ms_0}{f_0})$ for spatially coherent aperture fields to be

$$B_H = \frac{f_0}{2Ms_0 B} = \frac{1}{Ms_0}\left(\frac{f_0}{\Delta f}\right) \tag{3-71}$$

For white-light applications, $\frac{\Delta f}{f_0} \simeq 0.275$ and the effective spatial bandwidth of the spatial low-pass filter $H(\zeta)$ is on the order of

$$B_H \simeq \frac{3.636}{Ms_0} \tag{3-72}$$

or, in other words, the spatial frequency content of the sheared broadband fields $u_a(M(\bar{r}_d - \bar{s}_0))$ and $u_a(M(\bar{r}_d + \bar{s}_0))$ is limited to 3.6 times the reciprocal shear distance Ms_0 measured in the aperture plane.

Since the spatial field $u_a(\bar{r}_a)$ is complex, $H(\zeta)$ filters both real and imaginary quadratures of the sheared fields. The phase measurement derived from Eq (3-43), however, is expressed in terms of the magnitude $\hat{A}$ and phase $\hat{\phi}$ of the filtered spatial part of the aperture field envelope. The specific form of the distortion introduced into the measured aperture phase $\hat{\phi}$ by the filtering process cannot, in general, be determined for arbitrary forms of $\phi(\bar{r}_a)$. At this point, it will suffice to say that the phase of a white-light field measured by the AC shearing interferometer is the phase of a <u>filtered</u> aperture field--the filtering being introduced by diffraction of the white-light field by the interferometer's grating.

<u>Monochromatic Field Phase Measurement</u>. For spatially coherent aperture fields which are monochromatic, the correlation function $R_w(\tau)$ is flat so that $H(\zeta)$ is constant for all spatial frequencies. For the monochromatic case, then, no spatial filtering is introduced for any shear distance Ms_0. With no spatial filtering, the resulting interferometer output signal for x-shear is given by

$$i_d(\bar{r}_d,t) = \frac{2}{\pi} M^2[A(\bar{r}_a)]^2 \cos[\tfrac{1}{2}(\phi_+ + \phi_-) - \phi]$$

$$\sin[2\pi f_s t - \tfrac{1}{2}(\phi_- - \phi_+)] \qquad (3\text{-}73)$$

where $A(\bar{r}_a)$ is the amplitude of the aperture field at point $\bar{r}_a = M\bar{r}_d$

$$\phi = \phi(\bar{r}_a) \qquad (3\text{-}74)$$

is the phase of the spatial part of the aperture field

$$\phi_+ = \phi(\bar{r}_a - M\bar{s}_0) \qquad (3\text{-}75)$$

and

$$\phi_{-} = \phi(\bar{r}_a + M\bar{s}_0) \tag{3-76}$$

Note that for aperture phase functions $\phi(\bar{r}_a)$ which change at most linearly at each point in the aperture, the detector signal may be simplified further:

$$i_d(\bar{r}_d,t) = \frac{2}{\pi} M^2[A(\bar{r}_a)]^2 \sin(2\pi f_s t - \frac{1}{2}\Delta\phi) \tag{3-77}$$

where

$$\Delta\phi = \phi(\bar{r}_a + M\bar{s}_0) - \phi(\bar{r}_a - M\bar{s}_0) \tag{3-78}$$

is the linear change in phase over distance $\Delta x_a = 2Ms_0$ measured in the aperture plane for a monochromatic, spatially coherent, aperture field.

Refering to Figure 9, the local wavefront slope at a point $\bar{r}_{a_0} = (x_{a_0}, y_{a_0})$ in the aperture plane is approximately given by

$$\frac{\partial}{\partial x_a} \phi(x_a, y_{a_0})\bigg|_{x_a = x_{a_0}} = \frac{\phi(x_{a_0} + Ms_0, y_{a_0}) - \phi(x_{a_0} - Ms_0, y_{a_0})}{2Ms_0} \tag{3-79}$$

$$= \frac{\Delta\phi}{2Ms_0} \tag{3-80}$$

The validity of the approximation depends on how much the aperture phase actually fluctuates within a distance $\Delta x_a = 2Ms_0$. A detailed study of aperture phase fluctuations based on the phase statistics of turbulent atmosphere can be found in Ref 24.

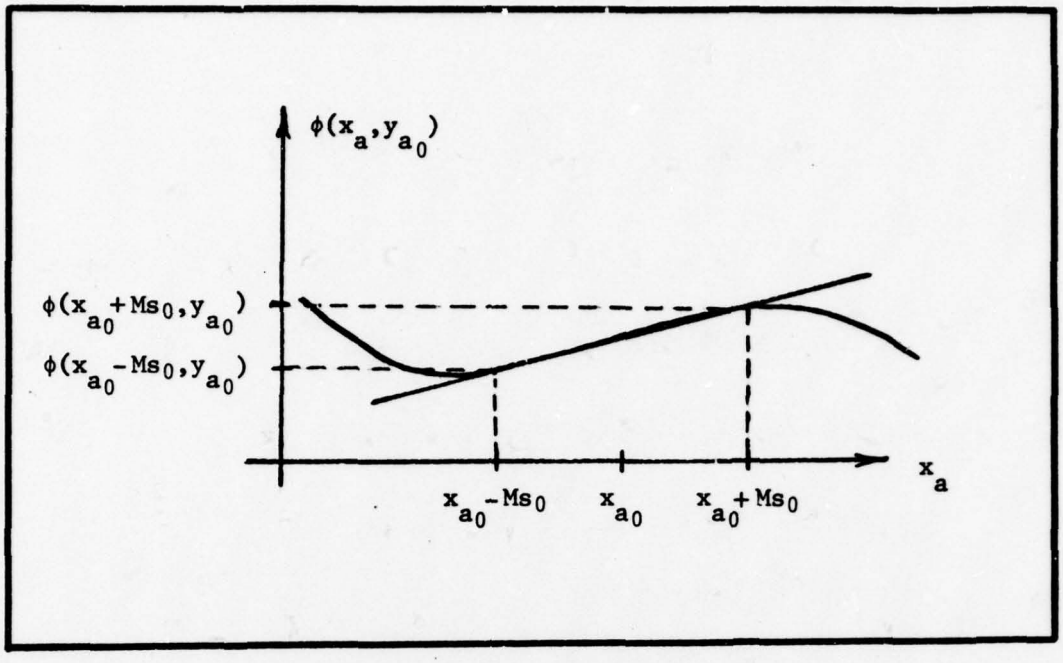

Figure 9. Aperture Phase $\phi(x_a, y_{a_0})$ for Fixed y_a Showing Calculation of Local Wavefront Slope

Therefore, for monochromatic light, the slope of the aperture field wavefront is given by Eq (3-79). Implicit assumptions are that the aperture field amplitude is constant, and the phase of the aperture field varies at most linearly over a distance $2Ms_0$ in the aperture plane.

Phase Measurement for Small Shear. For spatially coherent, white-light aperture fields where the shear Ms_0 is small enough that $R_w\left(\frac{f_x Ms_0}{f_0}\right)$ encloses all the spatial frequency components of $u_a(\bar{r}_a)$

$$B_a << B_H \simeq \frac{3.6}{Ms_0} \tag{3-81}$$

where B_a is the bandlimiting spatial frequency of $V_a(f_x, f_y)$, the spatial filtering effect of the shearing interferometer is negligible. For this case the filtered phases $\hat{\phi}_+$ and $\hat{\phi}_-$ defined in (3-45) and

(3-46) very closely approximate the actual phases ϕ_+ and ϕ_- of the sheared images of the aperture field envelope. The detector signal, then, is expressed by Eq (3-73) and the wavefront slope for x-shear is expressed by (3-80).

Phase Measurement for Large Shear. For spatially coherent, white-light aperture fields were the shear Ms_0 is large so that $R_w(\frac{f_x Ms_0}{f_0})$ is much narrower than the spatial frequency content of $u_a(\bar{r}_a)$

$$B_a >> B_H \simeq \frac{3.6}{Ms_0} \tag{3-82}$$

the phase measurement $\Delta\phi$ is lost completely. Using Eq (3-43) and approximating $R_w(\frac{f_x Ms_0}{f_0})$ by an impulse at $f_x = 0$ in Eq (3-66) yields

$$i_d(\bar{r}_d,t) = \frac{2B_H}{\pi} M^2 A_0 A(\bar{r}_a)\cos(\phi-\phi_0)\sin(2\pi f_s t) \tag{3-83}$$

where

$$B_H = \frac{1}{Ms_0}(\frac{f_0}{\Delta f}) \tag{3-84}$$

$$A_0 = \left|\int dx_a\, u_a(x_a,y_a)\right| \tag{3-85}$$

is the amplitude of the aperture field averaged over x_a, and

$$\phi_0 = \arg\left[\int dx_a u_a(x_a,y_a)\right] \tag{3-86}$$

is the phase of the aperture field averaged over x_a.

Filtering Effects for Aperture Fields with Arbitrary Spatial Coherence

For broadband aperture field envelopes with a complex degree of coherence $\tilde{\mu}_a$, the first-order spatial filter for the $m = +1$ diffracted field order is given by Eq (3-59):

$$H_+\left(\frac{f_x Ms_0}{f_0}\right) = \int dv \tilde{\mu}_a\left(\frac{Ms_0}{f_0}(f_0+v)\right) S_w(v) \exp\left[-j2\pi\left(\frac{f_x Ms_0}{f_0}\right) v\right] \quad (3\text{-}87)$$

Note that although $\tilde{\mu}_a$ has arbitrary form, it is assumed to be stationary for all separations $\bar{r}_a - \bar{r}'_a$ in the interferometer aperture plane.

The spatial filtering function H_+ can be interpreted as a Fourier transform of a "windowed" version of the temporal power spectrum:

$$H_+\left(\frac{f_x Ms_0}{f_0}\right) = F_v\{\hat{S}_w(v)\} \quad (3\text{-}88)$$

where

$$\hat{S}_w(v) = \tilde{\mu}\left(\frac{Ms_0}{f_0}(f_0+v)\right) S_w(v) \quad (3\text{-}89)$$

is the windowed version of the power spectrum, and the transform is evaluated at $f_x Ms_0/f_0$. The windowing effect can be better visualized with the help of Figure 10, where the windowing is accomplished by a shifted copy of the complex degree of coherence $\tilde{\mu}_a$ as prescribed by Eq (3-87). The degree of coherence μ_a sketched in Figure 10 is equal to the modulus of the complex degree of coherence $\tilde{\mu}_a$ (Ref 14:510). The spatial filtering function H_+, then, is the Fourier transform of the windowed, or filtered, power spectrum sketched in Figure 10(b).

Similarly following Eq (3-62), the spatial filter for the $m = -1$ diffracted order is the <u>inverse</u> Fourier transform of the windowed power spectrum $\hat{S}_w(v)$ defined by Eq (3-89)

$$H_-\left(\frac{f_x Ms_0}{f_0}\right) = F_v^{-1}\{\hat{S}_w(v)\} \quad (3\text{-}90)$$

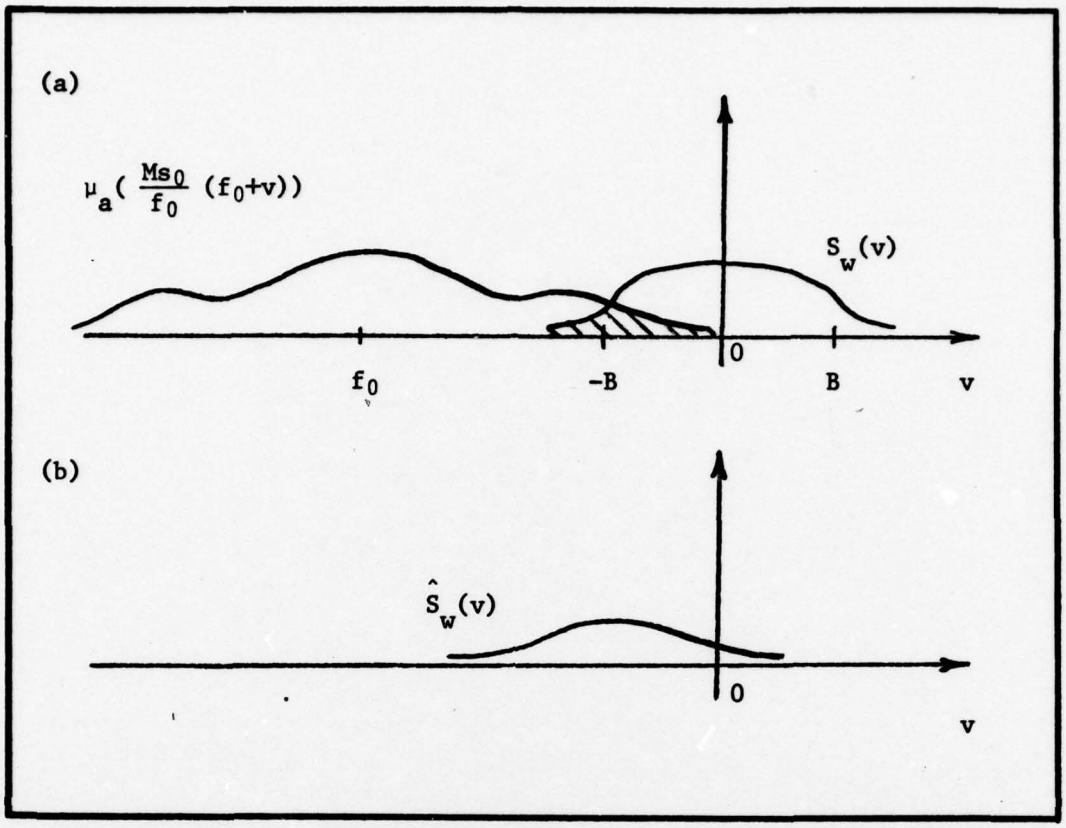

Figure 10. Windowing Effect of Degree of Coherence μ_a on the Temporal Power Spectrum S_w : (a) Power Spectrum and Degree of Coherence, (b) Windowed Temporal Power Spectrum $\hat{S}_w(v)$

It can be seen from Eqs (3-88) and (3-90) that the specific form of the filtering processes H_+ and H_- are highly dependent on the complex degree of coherence of the aperture field. Whereas the spatial filtering arises from the broadband temporal characteristics of the field, the functional form of this filtering depends on the spatial coherence of the field as well.

In the next chapter the lateral shear AC interferometer is applied to the measurement of an aperture phase due to a broadband, incoherent source. It is found that for specific source radiance distributions the

the complex degree of coherence of the aperture field can be calculated explicitly, and the particular form of the spatial filtering functions, for aperture fields which are not assumed to be coherence separable can be calculated.

IV. WAVEFRONT MEASUREMENT FOR SPATIALLY INCOHERENT, TEMPORALLY BROADBAND SOURCES

The lateral shear AC interferometer described in Chapter III has been used as a wavefront sensor in real-time atmospheric compensation systems (Refs 7, 8, 9, and 10). In this application, the interferometer is required to measure the phase of the optical field envelope in its input aperture due to an extended, white-light source. This chapter describes the closed-loop operation of the lateral shear AC interferometer as a wavefront sensor for broadband, spatially incoherent, extended sources based on the free-space propagation model introduced in Chapter III. The residual effects of atmospheric turbulence are modeled as a multiplicative phase factor introduced at the aperture plane of the wavefront sensor for each temporal mode of the field expansion for a frozen state of turbulence.

Wavefront Sensor Output Signal

Consider two parallel planes P_s and P_a separated by distance Z as shown in Figure 11. Let P_s contain an immobile, diffuse source of finite spatial extent reflecting white light. Let plane P_a represent the input aperture and measurement plane of the interferometer wavefront sensor, so that Z is the range of the source in meters. Allowing the source field to be modeled as coherence separable, the white-light source field may be characterized over a finite time interval T by a modal expansion as in (2-30):

$$U_s(\bar{r}_s,t) = u_s(\bar{r}_s) \sum_n w_n e^{+j2\pi\frac{n}{T}t}$$

$$\text{for } -\frac{T}{2} < t < \frac{T}{2} \qquad (4\text{-}1)$$

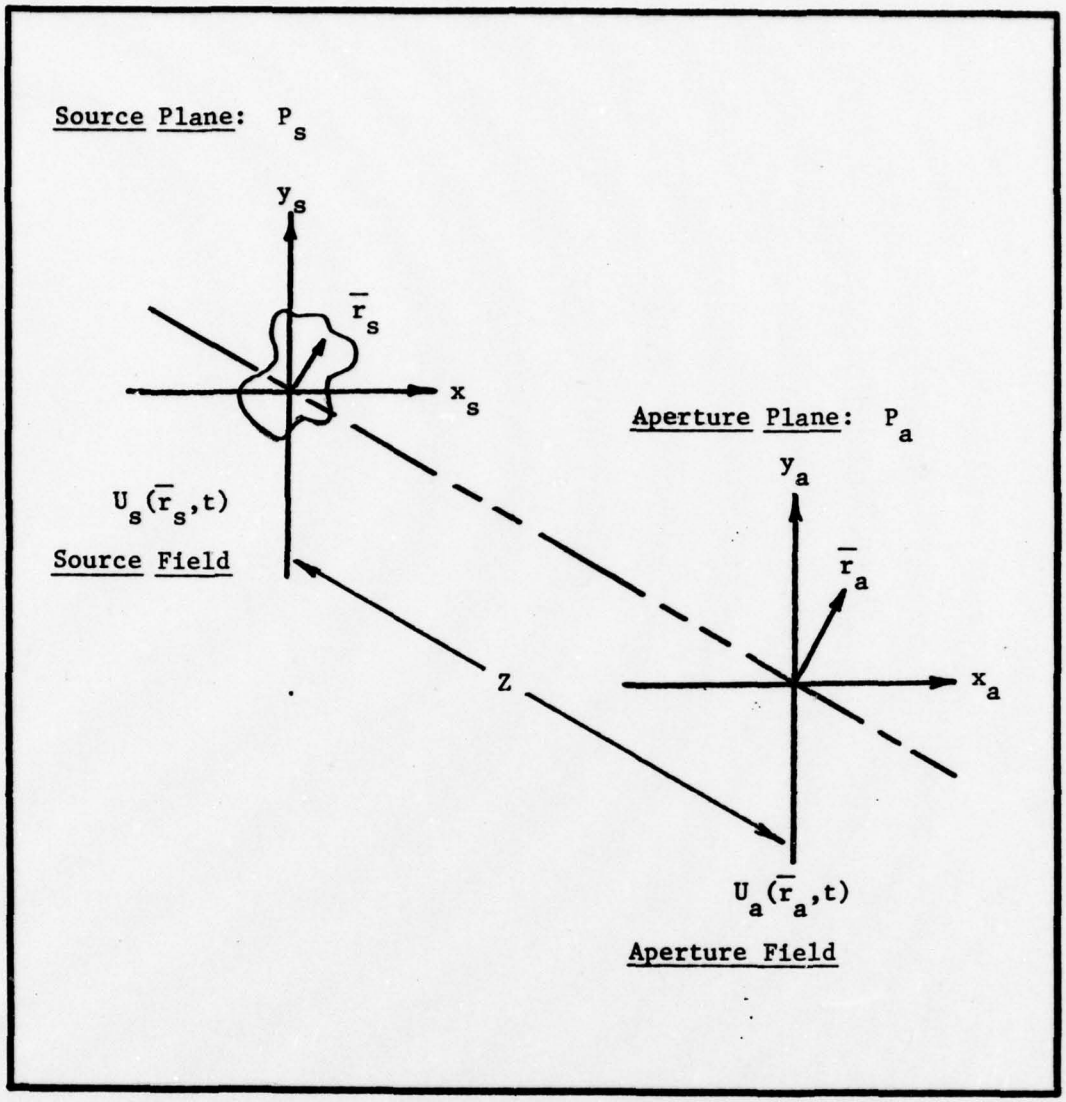

Figure 11. Free-Space Propagation Geometry for Extended, White-Light Source

where $u_s(\bar{r}_s)$ is the spatial part of the source field envelope, the sum over the temporal modes converges in mean-square.

If the source is sufficiently diffuse, the light reflected by it can be assumed to be spatially incoherent; the spatial correlation of the source field may be written (Ref 24:126 and Eq (2-55))

$$R_s(\bar{r}_s,\bar{r}_s') = u_s(\bar{r}_s)u_s^*(\bar{r}_s') = I_s(\bar{r}_s)\delta(\bar{r}_s-\bar{r}_s') \qquad (4\text{-}2)$$

where $I_s(\bar{r}_s)$ is defined to the radiant emittance (intensity) of the source in watts per meter squared.

Aperture Field. Using the free-space propagation model for broadband fields developed in Chapter II (Ref Eq (2-44)), the n^{th} temporal mode of the optical field $U_p(\bar{r}_a,t)$ just prior to the aperture plane P_a is given by

$$U_{pn}(\bar{r}_a,t) = u_{an}(\bar{r}_a)w_n e^{+j2\pi\frac{n}{T}t}$$

for $-\frac{T}{2} < t < \frac{T}{2}$ (4-3)

where

$$u_{an}(\bar{r}_a) = \frac{e^{jk_nZ}}{j\lambda_nZ}\int d\bar{r}_s\, u_s(\bar{r}_s)\exp[j\frac{k_n}{2Z}|\bar{r}_a-\bar{r}_s|^2] \qquad (4\text{-}4)$$

Note that since the field $U_p(\bar{r}_a,t)$ is the output field due to a spatially incoherent, coherence separable, broadband source field $U_s(\bar{r}_s,t)$, the spatial correlation of the field is given by Eq (2-57):

$$\Gamma_p(r_a,r_a') = \left\langle U_p(\bar{r}_a,t)U_p^*(\bar{r}_a',t)\right\rangle \qquad (4\text{-}5)$$

$$= (\frac{1}{\lambda_0Z})\sum_n \frac{1}{T}\xi^2(n)S_w(\frac{n}{T})e^{j\psi_n}$$

$$\int dr_s I_s(\bar{r}_s)\exp[-j\frac{k_n}{Z}\bar{r}_s\cdot(\bar{r}_a-\bar{r}_a')] \qquad (4\text{-}6)$$

where $\psi_n = \frac{\pi}{\lambda_0Z}\xi(n)(|r_a|^2 - |\bar{r}_a'|^2)$ (4-7)

Turbulence-Induced Phase Model. The effects of the atmosphere seriously degrade the imaging capability of optical systems in many applications. The resolution which is attainable for imaging through the earth's atmosphere is limited by warping of the isophase surfaces (phase distortion) and intensity variations across the wavefront caused by random fluctuations in the refractive index of air. For broadband optical fields, the phase distortion which is introduced can be thought of as a differential path length distortion introduced for all wavelengths, so that the phase distortion for each temporal mode measured in the aperture plane of the interferometer $\phi_{Tn}(\bar{r}_a)$ is

$$\phi_{Tn}(\bar{r}_a) = \frac{2\pi}{\lambda_n} \cdot \Delta Z(\bar{r}_a) \tag{4-8}$$

where $\Delta Z(\bar{r}_a)$ is the differential path length distortion introduced by a frozen atmospheric state for all temporal modes measured at a point $\bar{r}_a$ in the aperture plane.

To the extent that the phase fluctuations $\phi_{Tn}(\bar{r}_a)$ are correlated over the entire wavelength range $\Delta\lambda$ of the broadband source, the phase distortion for each temporal mode is approximately the same, and

$$\phi_{Tn}(\bar{r}_a) = \phi_{T_0}(\bar{r}_a)$$

$$\text{for } -BT < n < BT \tag{4-9}$$

where $\phi_{T_0}(\bar{r}_a)$ is the turbulence-induced phase distortion for $\lambda = \lambda_0$, which is the same for all wavelengths of light. For arbitrary spectral bandwidths, however, the phase distortion may not be assumed to be correlated for all modes of the field expansion (Ref 28:468).

Suppose that the n^{th} mode phase distortion is written as

$$\phi_{Tn}(\bar{r}_a) = \phi_{T_0}(\bar{r}_a) + \underset{\sim}{\phi}_{Tn}(\bar{r}_a) \tag{4-10}$$

where $\underset{\sim}{\phi}_{Tn}(\bar{r}_a)$ is the fluctuation of the turbulence-induced phase for each temporal mode about a mean phase, which is arbitrarily chosen to be that for λ_0. In general, $\underset{\sim}{\phi}_{Tn}(\bar{r}_a)$ will have values which differ greatly from $\phi_{T_0}(\bar{r}_a)$. If gross differential path length differences and wavefront tilt have been removed, as in the closed-loop operation of a real-time atmospheric correction device (Refs 7 and 9), the variation of the phase perturbation about $\phi_{T_0}(\bar{r}_a)$ for each mode will be about zero-mean over the range of the modal expansion:

$$\left\langle \underset{\sim}{\phi}_{Tn}(\bar{r}_a) \right\rangle = 0$$

for $-BT < n < BT$ (4-11)

where the expected value may be taken for each turbulent state of the atmosphere. Furthermore, if attention is restricted to points in the aperture plane such that

$$\text{Max}[|\bar{r}_a - \bar{r}_a'|] < \rho_0 \tag{4-12}$$

where ρ_0 is the spherical-wave coherence length for the space-to-earth propagation path (Refs 2:1376 and 26:1678), the correlation of the phase distortion for each monochromatic mode of the field expansion may be written (Refs 26:1683; 27:731; and 28:464-468)

$$\left\langle \underset{\sim}{\phi}_{Tn}(\bar{r}_a) \underset{\sim}{\phi}_{Tn}(\bar{r}_a') \right\rangle \simeq \left\langle \underset{\sim}{\phi}^2{}_{Tn}(\bar{r}_a) \right\rangle \tag{4-13}$$

This result is useful in the evaluation of the interferometer phase measurement for restricted operating conditions.

For real-world turbulence conditions, the random phase $\phi_{Tn}(\bar{r}_a)$ fluctuates with time causing scintillation. In order for the phase compensation system to operate properly, the response time of the imaging system, and so the wavefront sensor, must be short enough to respond to significant temporal fluctuations in the phase distortion. This requirement limits the measurement interval of the interferometer--and also the characterization interval of the broadband process T --tc less than about 10 milliseconds (Refs 26:1680 and 29:392). Note that this requirement does not prohibit the use of the modal propagation model since any practical measurement interval is still much greater than the reciprocal bandwidth of the temporal fluctuations of the white-light envelope (about 6.7×10^{-13} seconds).

Detector Plane Output Signal. Modeling the effects of atmospheric turbulence as a unit-modulus phase screen for each temporal mode, the n^{th} temporal mode of the field in the interferometer's aperture plane can be written

$$U_{an}(\bar{r}_a,t) = U_{pn}(\bar{r}_a,t)\exp[j\phi_{Tn}(\bar{r}_a)] \tag{4-14}$$

where $U_{pn}(\bar{r}_a,t)$ is the n^{th} mode of the aperture field due to an incoherent, broadband source given previously in Eq (4-3). Writing the broadband aperture field as the superposition of all temporal modes yields

$$U_a(\bar{r}_a,t) = \sum_n u_{an}(\bar{r}_a) w_n e^{j2\pi\frac{n}{T}t} e^{j\phi_{Tn}(\bar{r}_a)}$$

$$\text{for } -\frac{T}{2} < t < \frac{T}{2} . \tag{4-15}$$

Assuming that the random phase fluctuations of the turbulent atmosphere are independent of the source statistics, the spatial correlation of the aperture field can be calculated as follows:

$$\Gamma_a(\bar{r}_a,\bar{r}_a') = \left\langle U_a(\bar{r}_a,t)U^*(\bar{r}_a',t)\right\rangle \tag{4-16}$$

$$= \sum_n \left\langle u_{an}(\bar{r}_a)u^*_{an}(\bar{r}_a')\right\rangle$$

$$\left\langle \exp[j\phi_{Tn}(\bar{r}_a)-j\phi_{Tn}(\bar{r}_a')]\right\rangle$$

for $-\frac{T}{2} < t < \frac{T}{2}$ (4-17)

where $\left\langle u_{an}(\bar{r}_a)u^*_{an}(\bar{r}_a')\right\rangle = (\frac{1}{\lambda_n Z})^2 \frac{1}{T} S_w(\frac{n}{T})$

$$e^{j\psi_n}\int d\bar{r}_s\, I_s(\bar{r}_s)\exp[-j\frac{k_n}{Z} r_s\cdot(r_a-r_a')] \tag{4-18}$$

Note that for closed-loop operation of an atmospheric correction system, the statistics of the phase fluctuations and the modal expansion coefficients $\{w_n\}$ may not be completely uncorrelated. It is assumed that, for normal operation of the interferometer, the correlation of these two quantities is small enough that the correlation of the aperture field can be written as in Eq (4-17).

Without loss of generality, the turbulence-induced phase perturbation for each temporal mode may be represented as in Eq (4-10), and Eq (4-17) may be rewritten:

$$\Gamma_a(\bar{r}_a,\bar{r}_a') = \exp[j\phi_{T_0}(\bar{r}_a)-j\phi_{T_0}(\bar{r}_a')]$$

$$\sum_n \left\langle u_{an}(\bar{r}_a)u^*_{an}(\bar{r}_a')\right\rangle$$

$$\left\langle \exp[j\phi_{Tn}(r_a)-j\phi_{Tn}(r_a')]\right\rangle$$

for $-\frac{T}{2} < t < \frac{T}{2}$. (4-19)

For the case where the phase fluctuations $\phi_{Tn}(\bar{r}_a)$ are correlated over the temporal bandwidth of the source, $\underset{\sim}{\phi}_{Tn}(\bar{r}_a)$ is identically zero and the last expectation involving $\underset{\sim}{\phi}_{Tn}(\bar{r}_a)$ and $\underset{\sim}{\phi}_{Tn}(\bar{r}_a')$ will yield unity. For a real-time atmospheric correction system operating in closed-loop, $\underset{\sim}{\phi}_{Tn}(\bar{r}_a)$ represents the residual phase error associated with tracking the average phase $\phi_{T_0}(\bar{r}_a)$ of the aperture field.

As an example calculation, assume the closed-loop system is tracking well so that $\underset{\sim}{\phi}_{Tn}(\bar{r}_a)$ is zero-mean (Ref Eq (4-11)). Furthermore, assume $\underset{\sim}{\phi}_{Tn}(\bar{r}_a)$ is normally distributed so that the last expectation in Eq (4-19) can be written in terms of the characteristic function of a Gaussian random variable (Ref 30:159-160):

$$\left\langle \exp[j\underset{\sim}{\phi}_{Tn}(\bar{r}_a) - j\underset{\sim}{\phi}_{Tn}(\bar{r}_a')] \right\rangle = \exp[-\tfrac{1}{2}\sigma_\phi^2] \tag{4-20}$$

where

$$\sigma_\phi^2 = \left\langle [\underset{\sim}{\phi}_{Tn}(\bar{r}_a) - \underset{\sim}{\phi}_{Tn}(\bar{r}_a')]^2 \right\rangle \tag{4-21}$$

If the statistics of $\underset{\sim}{\phi}_{Tn}(\bar{r}_a)$ are stationary in P_a, the variance of the residual phase fluctuations σ_ϕ^2 may be further simplified:

$$\sigma_\phi^2 = 2\left\langle [\underset{\sim}{\phi}_{Tn}(r_a)]^2 \right\rangle [1-\rho(|r_a - r_a'|)] \tag{4-22}$$

where

$$\rho(|\bar{r}_a - \bar{r}_a'|) = \frac{\left\langle \underset{\sim}{\phi}_{Tn}(\bar{r}_a)\underset{\sim}{\phi}_{Tn}(\bar{r}_a') \right\rangle}{\left\langle [\underset{\sim}{\phi}_{Tn}(\bar{r}_a)]^2 \right\rangle} \tag{4-23}$$

Furthermore, if the phase measurement is restricted to regions in the aperture satisfying Eq (4-12), $\rho(|\bar{r}_a - \bar{r}_a'|)$ is nearly one for all points in the aperture and the expectation written in Eq (4-20) is nearly unity.

The above discussion has intended to demonstrate that for the restricted cases discussed above, namely (1) the phase fluctuations $\phi_{Tn}(\bar{r}_a)$ are correlated over the entire wavelength range of the source emission and (2) the residual phase error in a closed-loop phase-compensation system is small, the spatial correlation of the aperture field may be written

$$\Gamma_a(\bar{r}_a,\bar{r}_a) = \exp[j\phi_{T_0}(\bar{r}_a)-j\phi_{T_0}(\bar{r}_a)] \sum_n \left\langle u_{an}(\bar{r}_a)u^*_{an}(\bar{r}_a)\right\rangle \tag{4-24}$$

Substituting Eq (4-24) into the result for the interferometer output signal derived in Chapter III (Ref Eq (3-30)), the x-channel output signal may be calculated and is written on the next page in Eq (4-25). Henceforth it will be assumed that conditions are such that the phase which is measured by the interferometer represents the wavelength-independent phase $\phi_{T_0}(\bar{r}_a)$.

Eq (4-25) gives the x-channel output signal of the interferometer wavefront sensor due to a broadband, incoherent source viewed through atmospheric turbulence. Each temporal mode enclosed by the first real operator is a result of the coherent addition of the zero and +1 diffracted field orders, and represents the positive-shear term for each temporal mode. The sum of these terms expresses the superposition of all positive shear modes for the white-light interference pattern. Similarly, each mode enclosed by the second real operator is the result of the zero and -1 field orders and is called the negative-shear mode.

A few general comments can be made about the wavefront sensor output signal at this time:

$$i_d(\bar{r}_d,t) = \frac{M^2}{\pi(\lambda_0 Z)^2}\ \mathrm{Re}\{\exp[-j(2\pi f_s t - \tfrac{\pi}{2})]\exp[-j\tfrac{k}{Z}M^2 s_0 x_d]$$

$$\exp[-j\phi_{T_0}(M\bar{r}_d)]$$

$$\int d\bar{r}_s I_s(\bar{r}_s)\exp[+j\tfrac{k_0}{Z}Ms_0 x_s]$$

$$\frac{1}{T}\sum_n \xi^2(n) S_w(\tfrac{n}{T})\exp[j\pi\frac{M^2}{\lambda_0 Z}\ \frac{s_0^2}{\xi(n)}\ ]$$

$$\exp[j\phi_{T_0}(M(\bar{r}_d-\bar{s}_0))]\}$$

$$+\frac{M^2}{\pi(\lambda_0 Z)^2}\ \mathrm{Re}\{\exp[+j(2\pi f_s t - \tfrac{\pi}{2})]\ \exp[+j\tfrac{k}{Z}M^2 s_0 x_d]$$

$$\exp[-j\phi_{T_0}(M\bar{r}_d)]$$

$$\int d\bar{r}_s I_s(\bar{r}_s)\exp[-j\tfrac{k_0}{Z}Ms_0 x_s]$$

$$\frac{1}{T}\sum_n \xi^2(n) S_w(\tfrac{n}{T})\exp[j\pi\frac{M^2}{\lambda_0 Z}\ \frac{s_0^2}{\xi(n)}\ ]$$

$$\exp[j\phi_{T_0}(M(\bar{r}_d+\bar{s}_0))]\}$$

for $-\frac{T}{2} < t \leq \frac{T}{2}$ (4-25)

(1) All modes of the detector signal are modulated at the fundamental frequency f_s. If the wideband temporal process $w(t)$ is characterized over an interval T much shorter than the turbulence-induced phase fluctuations, the phase-front across the aperture may be considered frozen, and no additional frequency modulation is introduced.

(2) For each positive-shear term, the total spatial effect of the source radiance is confined to an integral over the source intensity distribution. For the negative-shear terms, the effect is represented by a similar integral. The integrals are independent of temporal mode, so that the spatial chracteristics of the source are entirely separate from the broadband temporal effects of the source. This result is due to the coherence separability of the source field. The detailed effects of the source's spatial content are discussed at length later in this chapter.

(3) For positive and negative-shear modes, the total effect of the broadband nature of the field is contained in a sum over all contributing temporal modes. Each term in the sum is weighted by the power spectrum of the broadband process $w(t)$.

In the next section, the effects of the complex source radiance and the broadband spectrum are separated, and the wavefront sensor's phase measurement is derived from the interferometer's detector signal expressed in Eq (4-25).

Derivation of the Wavefront Sensor Phase Measurement

The interferometer wavefront sensor's phase measurement is contained in the detector signal $i_d(\bar{r}_d,t)$ expressed in (4-25). To make the analysis more intuitive, the spatial and broadband effects of the source can

be separated and written in more compact functional forms. Following this separation, the derivation of the interferometer phase measurement follows easily.

Contribution Due to Source Radiance Distributions. As pointed out in the previous section, the total effect of the source's spatial distribution is contained in two similar integrals over the source radiance (intensity) distribution. Define $\tilde{J}_s(f_x,f_y)$ to be the spatial Fourier transform of the source radiance distribution

$$\tilde{J}_s(f_x,f_y) = F_{x_s y_s}\{I_s(x_s,y_s)\} \tag{4-26}$$

Note that the integral over the source distribution in the negative-shear modes can be written

$$\tilde{J}_s(f_x,0) = \int dx_s \int dy_s I_s(\bar{r}_s)\exp[-j2\pi f_x x_s] \tag{4-27}$$

$$= F_{x_s y_s}\{I_s(x_s,y_s)\} \tag{4-28}$$

where the Fourier transform is evaluated at spatial frequencies $f_x = \frac{Ms_0}{\lambda_0 Z}$ and $f_y = 0$.

Let the transform of the source radiance distribution be written in polar form so that

$$\tilde{J}_s(f_x,f_y) = J_s(f_x,f_y)\exp[j\psi_s(f_x,f_y)] \tag{4-29}$$

where $$J_s(f_x,f_y) = |\tilde{J}_s(f_x,f_y)| \tag{4-30}$$

is the magnitude and

$$\psi_s(f_x,f_y) = \arg[\tilde{J}_s(f_x,f_y)] \tag{4-31}$$

is the phase of the transform of the source radiance distribution. Using Eq (4-31), the integral (4-27) may be represented

$$\tilde{J}_s(f_x,0) = J_s(f_x,0)\exp[j\psi_s(f_x,0)] \tag{4-32}$$

where $f_x = \frac{Ms_0}{\lambda_0 Z}$.

Since the intensity distribution of the source $I_s(\bar{r}_s)$ is a real function of the source coordinates, the inverse Fourier transform of the source distribution is equal to the complex conjugate of the Fourier transform of the source distribution (Ref 31:28):

$$F^{-1}_{f_x f_y}\{I_s(\bar{r}_s)\} = \tilde{J}^*_s(f_x,f_y) \tag{4-33}$$

Using this notation, the integral over the positive-shear modes in Eq (4-25) may be written

$$\tilde{J}^*_s(f_x,0) = \int d\bar{r}_s I_s(\bar{r}_s)\exp[j2\pi f_x x_s] \tag{4-34}$$

$$= J_s(f_x,0)\exp[-j\psi_s(f_x,0)] \tag{4-35}$$

where $f_x = \frac{Ms_0}{\lambda_0 Z}$.

Contribution Due to Broadband Emission. Consider the sum over all the positive-shear temporal modes defined below:

$$\tilde{Q}(M(\bar{r}_d-\bar{s}_0)) = \frac{1}{T}\sum_n \xi^2(n) S_w(\tfrac{n}{T})\exp[j\pi\frac{M^2 s_0^2}{\lambda_0 Z\xi(n)}]$$

$$\exp[j\phi_{T_0}(M(\bar{r}_d-\bar{s}_0\xi^{-1}(n)))]$$

for $-\frac{T}{2} < t < \frac{T}{2}$. (4-36)

Using the binonial expansion for $\xi^{-1}(n)$ and approximating the sum by the first two terms allows (4-36) to be written

$$\tilde{Q}(M(\bar{r}_d-\bar{s}_0)) = \exp[j\frac{\pi M^2 s_0^2}{\lambda_0 Z}]\ \frac{1}{T}\sum_n \xi^2(n)S_w(\frac{n}{T})$$

$$\exp[j2\pi(\frac{M^2 s_0^2}{Zc})\frac{n}{T}]\ \exp\{j\phi_{T_0}[M(\bar{r}_d-\bar{s}_0(1+\frac{n}{f_0 T}))]\}$$

for $-\frac{T}{2} < t < \frac{T}{2}$. (4-37)

Performing the same approximation on the <u>negative-shear</u> modes yields

$$\tilde{Q}(M(\bar{r}_d+\bar{s}_0)) = \exp[j\frac{\pi M^2 s_0^2}{\lambda_0 Z}]\ \frac{1}{T}\sum_n \xi^2(n)S_w(\frac{n}{T})$$

$$\exp[j2\pi(\frac{M^2 s_0^2}{Zc})\frac{n}{T}]\ \exp\{j\phi_{T_0}[M(\bar{r}_d+\bar{s}_0(1+\frac{n}{f_0 T}))]\}$$

for $-\frac{T}{2} < t < \frac{T}{2}$. (4-38)

Furthermore, let the positive- and negative-shear terms be written in polar form so that

$$\tilde{Q}(M(\bar{r}_d-\bar{s}_0)) = \exp[j\pi\frac{M^2 s_0^2}{\lambda_0 Z}]\hat{A}_T(M(\bar{r}_d-\bar{s}_0))$$

$$\exp[j\hat{\phi}_T(M(\bar{r}_d-\bar{s}_0))] \qquad (4\text{-}39)$$

and

$$\tilde{Q}(M(\bar{r}_d+\bar{s}_0)) = \exp[j\pi \frac{M^2 s_0^2}{\lambda_0 Z}] \hat{A}_T(M(\bar{r}_d+\bar{s}_0))$$

$$\exp[j\hat{\phi}_T(M(\bar{r}_d+\bar{s}_0))]$$

(4-40)

It is shown in a later section that for white-light, incoherent source fields, the lateral shear AC interferometer causes the diffracted aperture field orders to be spatially filtered. The amplitude and phase of the filtered aperture field are identified by "hats."

Interferometer Phase Measurement. Substituting the defined relations (4-32), (4-35), (4-39), and (4-40) into the x-channel output signal given in (4-25) yields

$$i_d(\bar{r}_d,t) = \frac{M^2}{\pi(\lambda_0 Z)^2} J_s(f_x,0)\hat{A}_T(M(\bar{r}_d-\bar{s}_0)) \; \mathrm{Re}\{\exp[-j(2\pi f_s t - \frac{\pi}{2})]$$

$$\exp[-j2\pi \frac{M^2 s_0}{\lambda_0 Z}(x_d - \frac{s_0}{2})]\exp[-j\psi_s(f_x,0)]$$

$$\exp[j\hat{\phi}_T(M(\bar{r}_d-\bar{s}_0))-j\phi_{T_0}(M\bar{r}_d)]\}$$

$$+ \frac{M^2}{\pi(\lambda_0 Z)^2} J_s(f_x,0)\hat{A}_T(M(\bar{r}_d+\bar{s}_0)) \; \mathrm{Re}\{\exp[j(2\pi f_s t - \frac{\pi}{2})]$$

$$\exp[+j2\pi \frac{M^2 s_0}{\lambda_0 Z}(x_d - \frac{s_0}{2})]\exp[+j\psi_s(f_x,0)]$$

$$\exp[j\hat{\phi}_T(M(\bar{r}_d+\bar{s}_0))-j\phi_{T_0}(M\bar{r}_d)]\}$$

for $-\frac{T}{2} < t < \frac{T}{2}$ (4-41)

where $f_x = \frac{Ms_0}{\lambda_0 Z}$.

If the amplitudes of the spatially filtered orders are assumed to be equal over the distance of shear for each point in the detector plane

$$\hat{A}_T(M\bar{r}_d) \simeq \hat{A}_T(M(\bar{r}_d - \bar{s}_0)) \tag{4-42}$$

$$\simeq \hat{A}_T(M(\bar{r}_d + \bar{s}_0)) \tag{4-43}$$

both positive- and negative-shear terms in Eq (4-41) may be combined:

$$i_d(\bar{r}_d,t) = \frac{2M^2}{\pi(\lambda_0 Z)} J_s\left(\frac{Ms_0}{\lambda_0 Z},0\right)\hat{A}_T(M\bar{r}_d) \cos\left[\frac{1}{2}(\hat{\phi}_T^+ + \hat{\phi}_T^-) - \phi_{T_0} - \theta_s\right]$$

$$\sin\left[2\pi f_s t + \frac{1}{2}(\hat{\phi}_T^- - \hat{\phi}_T^+)\right.$$

$$\left. + \psi_s\left(\frac{Ms_0}{\lambda_0 Z}, 0\right) + \theta_d\right] \tag{4-44}$$

where

$$\hat{\phi}_T^+ = \hat{\phi}_T(M(\bar{r}_d - \bar{s}_0)) \tag{4-45}$$

$$\hat{\phi}_T^- = \hat{\phi}_T(M(\bar{r}_d + \bar{s}_0)) \tag{4-46}$$

$$\phi_{T_0} = \phi_{T_0}(M\bar{r}_d) \tag{4-47}$$

$$\theta_s = \frac{k_0}{2Z}(Ms_0)^2 \tag{4-48}$$

$$\theta_d = \frac{k_0}{Z} M^2 s_0 x_d \tag{4-49}$$

If the amplitudes of the spatially filtered orders are <u>not</u> equal over the distance of shear, the resulting detector signal is represented as the sum of two phasors as discussed in Chapter III (see Figure 8). In Eqs

(4-42) and (4-43), however, the filtered amplitudes $\hat{A}_T(M(\bar{r}_d-\bar{s}_0))$ and $\hat{A}_T(M(\bar{r}_d+\bar{s}_0))$ represent the amplitude of the diffracted and filtered aperture phase $\exp[j\phi_{T_0}(\bar{r}_a)]$ introduced by atmospheric turbulence. Since this phase term is assumed to have unit modulus for all points in the aperture plane, any sheared and filtered version of this filter will be equal to any other filtered version so long as the filtering effects are identical. In a later section it is shown that the amplitude of the filtered aperture field is in fact the same for either the $m = 1$ or $m = -1$ diffracted order.

Therefore, Eq (3-44) represents the interferometer output signal for x-shear for spatially incoherent, white-light sources viewed through atmospheric turbulence subject to the operating conditions discussed earlier. Note that all effects of the source's radiance distribution are contained in a multiplicative attenuation term $J_s(f_x,0)$ and an additive phase term $\psi_s(f_x,0)$. The effect of the diffraction of broadband light affects the phase measurement by filtering the measured phases $\hat{\phi}_T^+$ and $\hat{\phi}_T^-$, and attenuating the carrier by an amount $\hat{A}_T(M\bar{r}_d)$. The effects of source radiance distribution and broadband emission spectrum are discussed in the next two sections.

As defined in Eq (4-31), $\psi(f_x,0)$ is the phase of the spatial Fourier transform of the source radiance distribution evaluated at spatial frequencies $f_x = \frac{Ms_0}{\lambda_0 Z}$ and $f_y = 0$. Since the source distribution is always positive and real, $\psi_s(f_x,0)$ is an odd function of f_x and represents a constant phase offset in Eq (4-44) for any non-zero shear value. The size of this phase error depends on the specific radiance distribution of the source and the value of $f_x = \frac{Ms_0}{\lambda_0 Z}$.

In addition to the effects mentioned above, two additional phase terms θ_s and θ_d appear. Whereas $\hat{\phi}_T^+$, $\hat{\phi}_T^-$, and ϕ_{T_0} are representative of the turbulence-induced phase-front introduced at the aperture plane, the additional phase terms θ_s and θ_d represent the quadratic phase of a spherical wave eminating from a point source located at $\bar{r}_s = (0,0)$ in the source plane.

Measurement of Turbulence-Induced Phase. The total phase of the sinusoidal signal modulated at frequency f_s is the sum of three phases: (1) the differential aperture phase due to atmospheric turbulence $\frac{1}{2}(\hat{\phi}_T^- - \hat{\phi}_T^+)$, (2) the phase of spatial Fourier transform of the source radiance distribution $\psi_s(f_x,0)$, and (3) a quadratic phase θ_d. If the interferometer is set up to measure the slope of the turbulence-induced aperture phase, the post-detection processing of the interferometer output signal must be designed to extract the phase due to the first effect $(\hat{\phi}_T^- - \hat{\phi}_T^+)$, alone. Assuming signal processing has extracted the differential phase

$$\Delta\hat{\phi}_T = \hat{\phi}_T^- - \hat{\phi}_T^+ \tag{4-50}$$

the measured wavefront slope due to atmospheric turbulence for x-shear is

$$\frac{\partial}{\partial x_a}\phi_T(x_a,y_{a_0})\bigg|_{x_a=x_{a_0}} \simeq \frac{\hat{\phi}_T(x_{a_0}+Ms_0,y_{a_0}) - \hat{\phi}_T(x_{a_0}-Ms_0,y_{a_0})}{2Ms_0} \tag{4-51}$$

$$= \frac{\Delta\hat{\phi}_T}{2Ms_0} \tag{4-52}$$

where $\Delta\hat{\phi}_T$ is the differential turbulence-induced phase measured by the interferometer. The effect to which the actual wavefront phase $\Delta\phi_{T_0}$ is spatially filtered to yield $\Delta\hat{\phi}_T$ is discussed in a later section.

Visibility Limitations of Extended Source Distributions

In Eq (4-44) it is seen that the total effect of the source radiance (intensity) distribution on the aperture phase measurement is contained in the amplitude and phase of $\tilde{J}_s(f_x,0)$ defined by Eq (4-27):

$$\tilde{J}_s(f_x,0) = \int d\bar{r}_s I_s(\bar{r}_s) \exp[-j2\pi f_s x_s] \qquad (4\text{-}53)$$

where $f_x = \frac{Ms_0}{\lambda_0 Z}$.

The integral over x_s represents the spatial Fourier transform of the x-variations of the source intensity, evaluated at a spatial frequency $f_x = \frac{Ms_0}{\lambda_0 Z}$; the integral over y_s gives the total intensity along the y-direction for each x_s .

The result given in Eq (4-53) represents the mutual intensity (Ref 14:508) of light at two points in the aperture plane due to a quasi-monochromatic source emitting radiation near wavelength λ_0 . The points in the aperture are separated in the x-direction by distance $\Delta x_a = Ms_0$, with no separation in the y-direction.

The magnitude of $\tilde{J}_s(f_x,0)$ corresponds to the degree of coherence of the aperture field (Ref 14:510) which is defined to be the absolute value of the normalized Fourier transform of the source intensity distribution:

$$\mu_a(\bar{r}_a,\bar{r}_a') = \left| \frac{\int d\bar{r}_s I_s(\bar{r}_s) \exp -j\frac{2\pi}{\lambda_0 Z}(x_a x_s + y_a y_s)}{\int d\bar{r}_s I_s(\bar{r}_s)} \right| \qquad (4\text{-}54)$$

where $\mu_a(\bar{r}_a,\bar{r}_a')$ is the degree of coherence of the light at two points $\bar{r}_a$ and $\bar{r}_a'$ in the aperture plane.

If the amplitudes of the two sheared field orders are equal--as expressed in Eqs (4-42) and (4-43)--then $J_s(f_x,0)$ is related to the fringe visibility (Ref 14:507-508) of the interference fringes at the detector plane:

$$\gamma(M\bar{s}_0) = \left| \frac{J_s(f_x,0)}{\int d\bar{r}_s \; I_s(\bar{r}_s)} \right| \tag{4-55}$$

where $\gamma(M\bar{s}_0)$ is the fringe visibility of the interference fringes for two points in the aperture plane separated by distance Ms_0 in the x-direction with no separation in the y-direction, and $0 \leq \gamma(Ms_0) \leq 1$ for any shear. Note that for the case of a point source, the fringe visibility is unity for all shear values. For any extended source, however, the fringe visibility depends on the specific source radiance distribution and the shear distance chosen.

Clearly, $J_s(f_x,0)$ is proportional to the amplitude of the interferometer output signal for x-shear, and must be maintained at a significant value for the interferometer signal to be detected and the phase information to be extracted. The effects of shear distance s_0 on the fringe visibility are considered below for the case of uniform and complex extended source radiance distributions.

Uniform Source Distributions. The visibility of the interferometer fringe pattern for x-shear is the normalized Fourier transform of the source intensity distribution as expressed in Eq (4-55). As an example, consider uniform source with a square intensity distribution with width W meters and intensity I_0 watts per meter squared. The interferometer fringe visibility can be calculated from Eq (4-55):

$$\gamma_W(\overline{Ms}_0) = \left| \operatorname{sinc}\left[\pi\left(\frac{Ms_0}{\lambda_0 Z}\right)W\right] \right| \qquad (4\text{-}56)$$

where $\operatorname{sinc}(x) = \sin(x)/x$. The fringe visibility γ_W of the square source is plotted as a function of shear distance Ms_0 in Figure 12.

For a uniform square source, then, the interference fringe visibility generally drops off as the shear distance increases. To guarantee that significant fringe visibility is maintained, the shear is selected so that $\gamma_W(\overline{Ms}_0)$ is evaluated within the main lobe of the sinc (·) function:

$$Ms_0 < \frac{\lambda_0}{\alpha} \qquad (4\text{-}57)$$

where $\alpha = W/Z$ is the angular subtense of the source.

For uniform, circular source distributions the fringe visibility is related to a first order Bessel function, and a result similar to Eq (4-57) for circular sources can be shown to be

$$Ms_0 < 1.22\,\frac{\lambda_0}{\alpha} \qquad (4\text{-}58)$$

where $\alpha = D/Z$ is the angular subtense of the circular source.

Therefore, the restriction placed on shear distance for circular sources with angular subtense $\alpha = D/Z$ is on the same order as (4-57) for a square target of equal angular subtense.

Complex Source Distributions. Sources of interest to imaging systems generally contain some degree of fine structure. Sources with structure contain more high spatial frequency information than uniform sources, and cause the fringe visibility function $\gamma(\overline{Ms}_0)$ to have significant value

AD-A064 404 AIR FORCE INST OF TECH WRIGHT-PATTERSON AFB OHIO SCH--ETC F/G 20/6
COHERENCE PROPERTIES OF BROADBAND OPTICAL FIELDS WITH APPLICATI--ETC(U)
DEC 78 P S IDELL

UNCLASSIFIED AFIT/GEO/EE/78-1 NL

2 OF 2
AD
A064 404

END
DATE
FILMED
4-79
DDC

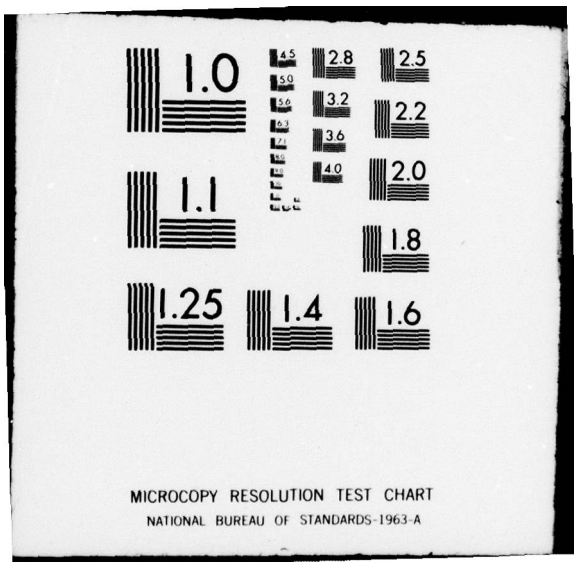
1.0
1.1
1.25
1.4
1.6
1.8
2.0
2.2
2.5
2.8
3.2
3.6
4.0
4.5
5.0
5.6
MICROCOPY RESOLUTION TEST CHART
NATIONAL BUREAU OF STANDARDS-1963-A

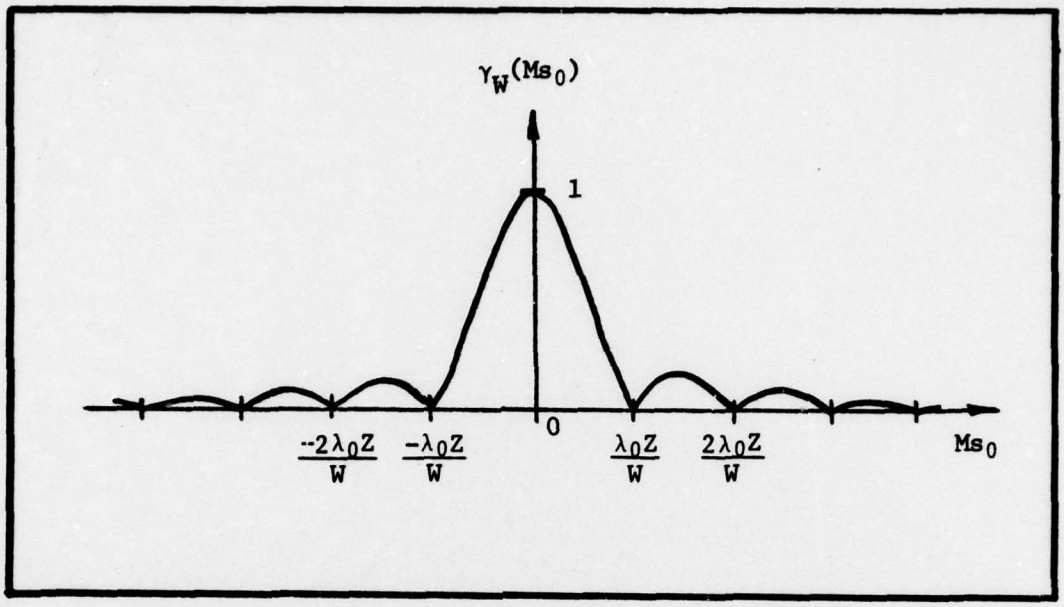

Figure 12. Fringe Visibility γ_W as a Function of Shear Distance for a Uniform Source of Width W

for large shear values. Although the visibility effects of each complex source must be considered separately, the general effect can be illustrated by the following example.

Consider a square source of width W having a periodic intensity distribution similar to a bar pattern with variations along the x-direction as shown in Figure 13. Note that the visibility function $\gamma_B(M\bar{s}_0)$ contains weighted copies of the visibility function of a square source $\gamma_W(M\bar{s}_0)$ located at $s_0 = m\frac{\lambda_0}{MX}$, where m is an integer. It is seen that periodic source distributions have a "coherence modulation" effection, due to the spatial frequency modulation properties of periodic source functions; and the fringe visibility can have significant value for shear distances much larger than those allowed by uniform sources.

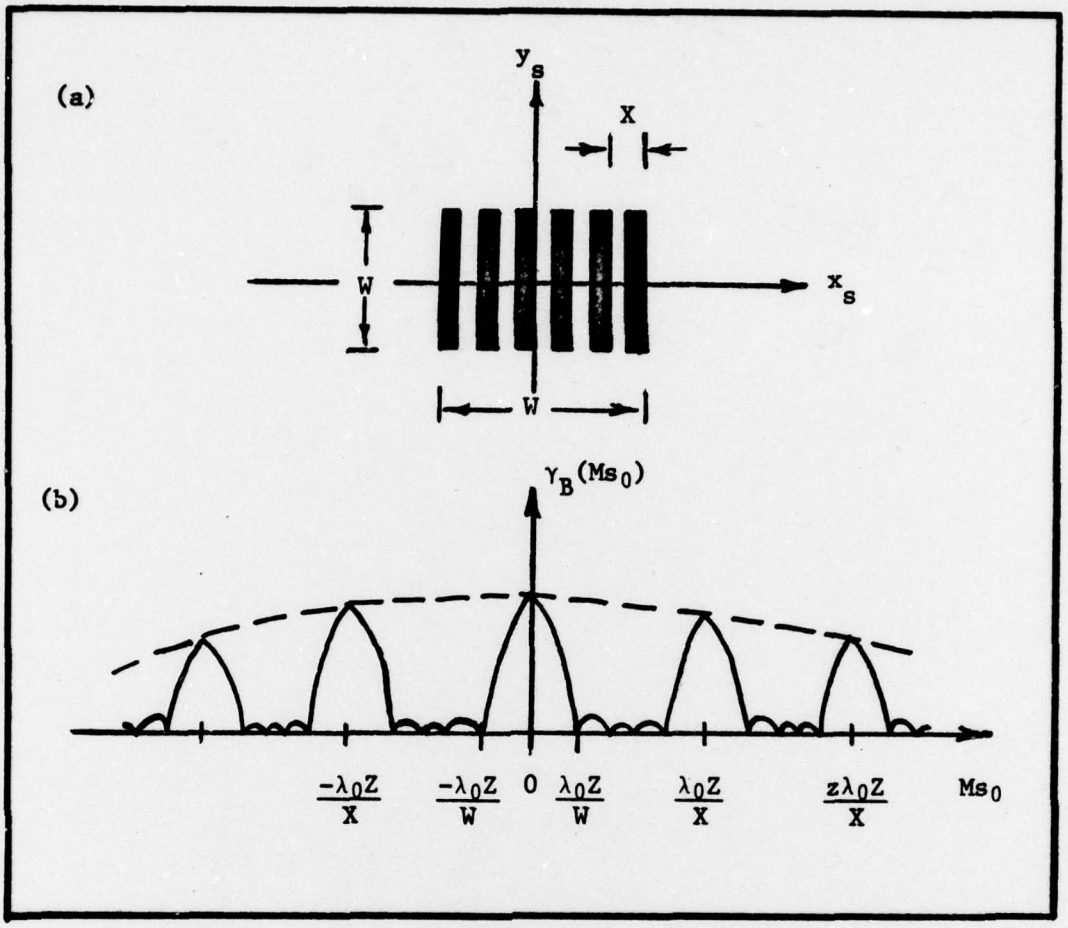

Figure 13. (a) Periodic Source Distribution and (b) Corresponding Fringe Visibility Function $\gamma(Ms_0)$ for x-shear of Ms_0

Since the total radiant power for any source is finite, the power is distributed among the many lobes of the fringe visibility function, and the magnitude of the fringe visibility at any shear may be neglibible. In any practical sense, then, the measurable fringe visibility is greatly dependent on total source radiance and the complexity of the source distribution.

Special Filtering Effects of Broadband Light

Consider the approximation to the sum of the positive-shear temporal modes written previously in Eq (4-37):

$$\tilde{Q}(M(\bar{r}_d-\bar{s}_0)) = \exp[j\theta_s]\,\frac{1}{T}\sum_n \xi^2(n)S_w(\tfrac{n}{T})\exp[j2\pi(\frac{M^2s_0^2}{Zc})\tfrac{n}{T}]$$

$$\exp\{j\phi_{T_0}[M(\bar{r}_d-\bar{s}_0(1+\tfrac{n}{f_0T}))]\}$$

$$\text{for } -\frac{T}{2}<t<\frac{T}{2}\,. \qquad (4\text{-}59)$$

Taking the spatial Fourier transform of (4-59) with respect to the aperture plane coordinates $x_a = Mx_d$ and $y_a = My_d$ yields

$$F_{x_a y_a}\{\tilde{Q}(M(\bar{r}_d-\bar{s}_0))\} = \exp[j\theta_s]\phi_{T_0}(f_x,f_y)\exp[-j2\pi f_x Ms_0]$$

$$\frac{1}{T}\sum_n \xi^2(n)S_w(\tfrac{n}{T})\exp[-j2\pi(\frac{f_x Ms_0}{f_0}-\frac{M^2s_0^2}{Zc})\tfrac{n}{T}]$$

$$\text{for } -\frac{T}{2}<t<\frac{T}{2} \qquad (4\text{-}60)$$

where $$\Phi_{T_0}(f_x,f_y) = F_{x_a y_a}\{\exp[j\phi_{T_0}(r_a)]\} \tag{4-61}$$

For broadband power spectra and long process characterization intervals the sum over temporal modes may be approximated by an integral:

$$F_{x_a y_a}\{\tilde{Q}(M(\bar{r}_d-\bar{s}_0))\} = \exp[j\theta_s]\Phi_{T_0}(f_x,f_y)\exp[-j2\pi f_x Ms_0]$$

$$\int dv\ \xi^2(v)S_w(v)\exp[-j2\pi\zeta_+ v] \tag{4-62}$$

where $$\zeta_+ = \frac{Ms_0}{f_0}\left(f_x - \frac{Ms_0}{\lambda_0 Z}\right) \tag{4-63}$$

and v has been substituted for $\frac{n}{T}$ as the integration variable. The integral over v in Eq (4-62) represents the first-order spatial filter for the $m = +1$ diffracted aperture field order given by Eq (3-87) where the complex degree of coherence of white-light aperture field has been calculated explicitly.

Following Eq (3-88) the first-order spatial filter affecting the $m = +1$ diffracted aperture phase $\exp[j\phi_{T_0}(\bar{r}_a)]$ is

$$H_+(\zeta_+) = F_v\{\xi^2(v)S_w(v)\} \tag{4-64}$$

For typical compensated imaging applications, sources are distant compared to the shear distance Ms_0. Assuming $\frac{Ms_0}{\lambda_0 Z}$ is small compared to the spatial bandwidth of H_+

$$B_H >> \frac{Ms_0}{\lambda_0 Z} \tag{4-65}$$

where B_H is the effective bandwidth of the spatial filter H_+, the first-order spatial filter can be written

$$H_+(\zeta) = F_v\{\xi^2(v)S_w(v)\} \tag{4-66}$$

where $\zeta = \frac{f_x M s_0}{f_0}$ as defined in Eq (3-60). Using results from Chapter II (Ref Eq (2-71)), Eq (4-66) can be written in terms of the first two derivatives of the temporal correlation function $R_w(\tau)$:

$$H_+(\zeta) = R_w(\zeta) + \frac{j}{\pi f_0}\frac{\partial}{\partial \zeta} R_w(\zeta) - \frac{1}{(2\pi f_0)^2}\frac{\partial^2}{\partial \zeta^2} R_w(\zeta) \tag{4-67}$$

Similarly, the sum over the <u>negative-shear</u> temporal modes can be approximated by an integral, and a filtering function for the $m = -1$ diffracted field order can be defined. Following Eqs (3-90) and (2-70),

$$H_-(\zeta) = F_v^{-1}\{\xi^2(v)S_w(v)\} \tag{4-68}$$

$$= R_w(\zeta) - \frac{j}{\pi f_0}\frac{\partial}{\partial \zeta} R_w(\zeta) - \frac{1}{(2\pi f_0)^2}\, 2\frac{\partial^2}{\partial \zeta^2} R_w(\zeta) \tag{4-69}$$

$$= H_T^*(\zeta) \tag{4-70}$$

Therefore, Eq (4-67) and its conjugate (4-89) represent, at least to first order, the form of the spatial filtering introduced into the interferometer phase measurement due to the diffraction of broadband light for the $m = +1$ and $m = -1$ diffracted orders. The spatial filtering function is similar to the "windowing" function $R_w(\cdot)$ discussed in Chapter II with regard to coherence length (Ref Eq (2-70)).

Indeed, if the power spectrum $S_w(f)$ is sufficiently narrow so that $\xi^2(n)$ may be closely approximated by unity, the filtering functions H_+

and H_- take on the form of the temporal correlation function:

$$H_+(\zeta) = H_-(\zeta) = R_w(\zeta) \tag{4-71}$$

Consider, for example, a bandlimited power spectrum $S_b(f)$ discussed in Chapter III (Ref Eq (3-70)). The effective bandwidth of the resulting spatial filter is on the order of

$$B_H \simeq \frac{1}{Ms_0} \left(\frac{f_0}{\Delta f}\right) \tag{4-72}$$

as defined in Eq (3-71). If the bandwidth of the spatial Fourier transform of the turbulence-induced aperture phase $\phi_{T_0}(f_x, f_y)$ is much less than B_H

$$B_\phi << B_H \simeq \frac{1}{Ms_0} \left(\frac{f_0}{\Delta f}\right) \tag{4-73}$$

where B is the spatial bandwidth of either real or imaginary quadrature of $\exp[j\phi_{T_0}(\bar{r}_a)]$, then the spatial filters introduce negligible filtering of the aperture phase field orders contributing to the AC interferometer pattern, and cause little distortion in the measured aperture phase.

In summary, then, for truly broadband optical fields with arbitrary power spectra, the form of the spatial filtering must be calculated from the discrete sum over temporal modes as in Eq (4-36). To first order, however, the spatial filtering can be calculated from derivatives of the broadband field correlation function as in Eqs (4-67) and (4-69).

V. CONCLUSION

Summary of Results

Coherence Model for Broadband Fields. A free-space propagation model for broadband optical fields was developed based on a Karhunen-Loéve (KL) expansion of the time-varying portion of a coherence separable, broadband optical envelope. Due to the linearity of the free-space channel, each temporal mode of the field expansion could be propagated individually, and the output broadband field could be computed as simply the superposition of all the individually propagated field modes. It was found that for broadband optical fields characterized over long time intervals, the eigenfunctions of the KL expansion were approximated by the complex exponentials of a Fourier series expansion over the same time interval. The eigenvalues of the modal expansion were found to be samples of the temporal power spectrum, sampled at the harmonic frequencies of the Fourier series expansion. Since the expansion coefficients of a KL expansion are uncorrelated, the calculation of output field correlation was facilitated. The output field correlation for coherence separable source fields was stated for special cases of source field coherence in Table I. The output field correlation due to coherence separable source fields was found to be, in general, not coherence separable (Ref Eq (2-47)).

Analysis of White-Light Interferometer. Application of the broadband propagation model to the lateral shear heterodyne interferometer showed that the position of the interference fringes detected by the interferometer was dependent on wavelength. This effect, caused by the

diffraction of the white-light aperture field by the interferometer's rotating grating, was shown to spatially filter the $m = 1$ and $m = -1$ diffracted field orders contributing the interference pattern. To first-order, the form of the spatial filter was shown to be given by a Fourier transform of the product of the broadband temporal power spectrum and a shifted version of the complex degree of coherence of the aperture field (Ref Eqs (3-87) and (3-89)). The measurement made by the interferometer was found to be related to the phase of the spatially filtered aperture field envelope. The interferometer wavefront measurement was specialized for spatially coherent aperture fields for large and small shear (Ref Eqs (3-83) and (3-77)).

Measurement of Turbulence-Induced Phase. The broadband field coherence model was applied to the application of the shearing interferometer as a wavefront sensor in a phase-compensated imaging system. It was argued that if the turbulence-induced phase fluctuations $\phi_{Tn}(\bar{r}_a)$ were correlated over the wavelength range of the source emission spectrum or the sensor operated in a closed-loop mode where the residual phase tracking errors were small, the turbulence-induced phase fluctuations could be modeled as a unit-modulus phase screen for all wavelengths of interest (Ref Eq (4-24)).

If the source was immobile and sufficiently diffuse, the source field could be modeled as being coherence separable. This model allows the visibility effects due to extended source radiance distribution and the spatial filtering effects due to broadband emission to be separated in the analysis of the interferometer. The visibility of the interference fringes was found to be proportional to the magnitude of the Fourier transform of the source radiance distribution as prescribed by the Van Cittert-Zernicke theorem (Ref 14:510) for quasi-monochromatic sources (Ref Eq (4-28)).

It was found that the phase measured by the interferometer for this application was due to the sum of three effects (Ref Eq (4-44)): (1) the turbulence-induced aperture phase perturbation, (2) the phase of the spatial Fourier transform of the source radiance distribution, and (3) the quadratic phase due to a point source at the source plane measured in the aperture plane. In order to measure the aperture phase due to atmospheric turbulence, signal processing must be designed to extract the first phase effect from the interferometer output signal. For typical compensated imaging situations it was found that to first order, the spatial filtering could be expressed in terms of the first two derivatives of the broadband temporal correlation function (Ref Eqs (4-67) and (4-69)).

Discussion and Suggestions for Further Study

In Chapter II a coherence model for the propagation of broadband optical fields was developed from a modal expansion of the time-varying part of the complex field envelope. Although the model was specifically applied to the analysis fo a white-light shearing interferometer in this paper, the application of this model may be extended to many broadband optical or infra-red systems for which the input fields can be assumed to be coherence separable. For example, the free-space propagation model (Eq (4-42)), the apochromatic lens result (Eq (3-7)), and the rotating diffraction grating model (Eq (3-13)) are particularly applicable to optical interferometric and measurement systems. Indeed, a broadband optical field can still be represented as a modal expansion if it is due to a source which can be assumed to be coherence separable (Ref Eq (2-42)) and the effects of the propagation medium can be considered to be frozen in time (Ref Eq (4-8)).

In Chapter III the lateral shear AC interferometer was analyzed for broadband aperture fields with arbitrary spatial coherence. Several assumptions were made which may further qualify the application or degrade the predicted performance of the wavefront sensor. First of all, all diffraction effects due to finite lens apertures and field stops were ignored. All optics were assumed to be perfectly transmissive for all wavelengths of interest and the lenses were assumed to be aberration-free and perfectly apochromatic. These effects must be studied in detail, or at least considered, for any practical application of a physically realizable wavefront sensor.

The interferometer output signal $i_d(\bar{r}_d,t)$ calculated in Chapters III and IV (Ref Eqs (3-43) and (4-44)) represents the time-varying interference pattern at each point in the detector plane modulated at f_s Hertz. No model for the photon/electron conversion of this white-light intensity pattern into an electrical signal was proposed, nor was a signal processing scheme suggested for the extraction of the aperture phase measurement $\Delta\phi$ from the detector plane output signals. It is recommended that a model for the detection of broadband radiation be incorporated into the analysis of the interference pattern (Eq 3-34) to determine what additional, if any, filtering effects are introduced into the wavefront measurement. Once these detected interferometer output signals are determined, several electronic processing schemes can be considered to provide the best aperture phase measurement (e.g., Refs 32, 33, and 34).

It was found that the shearing interferometer's operation for broadband fields causes the $m = +1$ and $m = -1$ diffracted aperture field orders contributing the detector plane interference pattern to

be spatially filtered. Whereas the filtering affects both real and imaginary quadratures of the complex aperture field envelope, the phase measurement, derived from the interferometer output signal (Eq (3-47)), represents the phase of a filtered complex field. Except for the special filtering cases studied--extremely wide filter (Eq (3-73) and extremely narrow filter (Eq (3-83))--the effect of spatial filtering on the detected aperture phase is extremely difficult to determine. The effects of filtering on the measured phase of phase modulated systems have been studied (e.g., Refs 35, 36, and 37), but are beyond the scope of this paper.

For the analysis of shearing interferometer wavefront measurement it was assumed that either the phase of the complex aperture field envelope was the same for all wavelengths of light or the interferometer was working in closed-loop with a real-time phase-correction system. The end result was that the interferometer adequately measured a phase which is common for all wavelengths when the residual phase errors are small. These assumptions were motivated by the fact that for the compensated imaging system considered in Chapter IV (Ref 7), atmospheric phase correction is accomplished by a single corrector--thus introducing the same compensation for all wavelengths. For more general active optic applications in which the wavefront correction is wavelength-dependent (e.g., Ref 12), the decomposition of the aperture phase into wavelength-dependent temporal modes, and the effect of this decomposition on the interferometer measurement, may be studied.

Bibliography

1. Jensen, N. Optical and Photographic Reconnaissance Systems. New York: John Wiley and Sons, Inc., 1968.

2. Fried, D. "Optical Resolution Through a Randomly Inhomogeneous Medium for Very Long and Very Short Exposures," Journal of the Optical Society of America, 56 (10):1372-1379 (October 1966).

3. Hufnagel, R. E. and N. R. Stanley. "Modulation Transfer Function Associated with Image Transmission Through Turbulent Media," Journal of the Optical Society of America, 54(1):52-61 (January 1964).

4. Muller, R. A. and A. Buffington. "Real-Time Correction of Atmospherically Degraded Telescope Images Through Image Sharpening," Journal of the Optical Society of America, 64(9):1200-1210 (September 1974).

5. Dicke, R. H. "Real-Time Correction of Telescope Seeing," Journal of the Optical Society of American, 65(10):1206 (October 1975).

6. Cathey, W. T., et al. "Compensation for Atmospheric Phase Effects at 10.6μ," Applied Optics, 9(3):701-707 (March 1970).

7. Hardy, J. W., et al. "Real-Time Atmospheric Compensation," Journal of the Optical Society of America, 67(3):360-369 (March 1977).

8. Wyant, J. C. "Use of an AC Heterodyne Lateral Shear Interferometer with Real-Time Wavefront Correction Systems," Applied Optics, 14(11): 2622-2626 (November 1975).

9. Hardy, J. W., et al. "Real-Time Phase Correction of Optical Imaging Systems," Digest of Technical Papers: Topical Meeting on Optical Propagation through Turbulence, Sponsored by the Optical Society of America, held at Boulder, Colorado, July 1974, Paper ThB1.

10. Hardy, J. W. "Active Optics: A New Technology for the Control of Light," Proceedings of the IEEE, 66(6):651-697 (June 1978).

11. Bridges, W. B., et al. "Coherent Optics Adaptive Techniques," Applied Optics, 13(2):291-300 (February 1974).

12. Mahajan, V. N. "Real-Time Correction Through Bragg Diffraction of Light by Sound Waves," Journal of the Optical Society of America, 65(3):271-278 (March 1975).

13. Hayes, C. L., et al. "Experimental Test of an Infrared Phase Conjugation Adaptive Array," Journal of the Optical Society of America, 67 (3):269-277 (March 1977).

14. Born, M. and E. Wolf. Principles of Optics (Fifth Edition). New York: Pergamon Press, 1975.

15. Gagliardi, R. M. and S. Karp. Optical Communications. New York: John Wiley and Sons, 1976.

16. VanTrees, H. Detection, Estimation and Modulation Theory, Part I. New York: John Wiley and Sons, 1968.

17. Courant, R. and D. Hilbert. Methods of Mathematical Physics, Volume I. New York: Interscience Publishers, Inc., 1953.

18. Riesz, F. and B. Sz.-Nagy. Functional Analysis. New York: Frederick Ungar Publishing Company, 1955.

19. Davenport, Jr., W. B. and W. L. Root. An Introduction to the Theory of Random Signals and Noise. New York: McGraw-Hill Book Company, 1958.

20. Goodman, J. W. Introduction to Fourier Optics. New York: McGraw-Hill Book Company, 1968.

21. Jenkins, F. A. and H. E. White. Fundamentals of Optics (Third Edition). New York: McGraw-Hill Book Company, 1957.

22. Beran, M. J. and G. B. Parrent. Theory of Partial Coherence. Redondo Beach, California: Society of Photo-Optical Instrumentation Engineers, 1974.

23. Ziemer, R. E. and W. H. Tranter. Principles of Communications: Systems, Modulation, and Noise. Boston: Houghton Mifflin Company, 1976.

24. Greenwood, D. P. and D. L. Fried. "Power Spectra Requirements for Wave-Front-Compensative Systems," Journal of the Optical Society of America, 66(3):193-200 (March 1976).

25. O'Neill, E. L. Introduction to Statistical Optics. Reading, Massachusetts: Addison-Wesley Publishing Company, Inc., 1963.

26. Fante, R. L. "Electromagnetic Beam Propagation in Turbulent Media," Proceedings of the IEEE, 63(12):1669-1692 (December 1975).

27. Fante, R. L. "Some Results on the Effect of Turbulence on Phase-Compensated Systems," Journal of the Optical Society of America, 66(7):730-735 (July 1976).

28. Shapiro, J. H. "Propagation-Medium Limitations on Phase-Compensated Atmospheric Imaging," Journal of the Optical Society of America, 66(5):460-469 (May 1976).

29. Greenwood, D. P. "Bandwidth Specification for Adaptive Optics Systems," Journal of the Optical Society of America, 67(3):390-393 (March 1977).

30. Papoulis, A. Probability, Random Variables and Stochastic Processes. New York: McGraw-Hill Book Company, 1965.

31. Lathi, B. P. Signals, Systems, and Communication. New York: John Wiley and Sons, Inc., 1965.

32. Fried, D. L. "Least Square Fitting a Wave-Front Distortion Estimate to an Array of Phase-Difference Measurements," Journal of the Optical Society of America, 67(3):370-375 (March 1977).

33. Hudgin, R. H. "Optimal Wave-Front Estimation," Journal of the Optical Society of America, 67(3):378-382 (March 1977).

34. Martone, P. J. "Signal Processing for Shearing Interferometer Measurements." Unpublished thesis. AFIT/GEO/EE/78-2. Wright-Patterson AFB: Air Force Institute of Technology, December 1978.

35. Bedrosian, E. and S. O. Rice. "Distortion and Crosstalk of Linearly Filtered Angle-Modulated Signals." Proceedings IEEE, 56(1):2-13 (January 1958).

36. Tue, H. H. "A New Approach to Computing Distortion of an FM Single-Tone Modulated Signal Due to Ideal Filtering," IEEE Transactions on Communications, 24(12):1317-1321 (December 1976).

37. Jeruchim, M. C. "Interference in Angle-Modulated Systems with Predetection Filtering," IEEE Transactions on Communications, 28(10):723-726 (October 1971).

VITA

Paul Steven Idell was born on 26 July 1955 in Pequannock Township, New Jersey. He graduated from Kinnelon High School in Kinnelon, New Jersey in 1973. He attended Lehigh University in Bethlehem, Pennsylvania, where he received a Bachelor of Science degree in Electrical Engineering in May 1977. Upon graduation, he received a commission in the United States Air Force through the AFROTC program. He entered active duty and the School of Engineering, Air Force Institute of Technology, in July 1977.

Permanent address: 7 Bubbling Brook Road
Kinnelon, New Jersey 07405

This thesis was typed by Elaine M. Tabbert.

UNCLASSIFIED

SECURITY CLASSIFICATION OF THIS PAGE (When Data Entered)

REPORT DOCUMENTATION PAGE		READ INSTRUCTIONS BEFORE COMPLETING FORM
1. REPORT NUMBER AFIT/GEO/EE/78-1	2. GOVT ACCESSION NO.	3. RECIPIENT'S CATALOG NUMBER
4. TITLE (and Subtitle) COHERENCE PROPERTIES OF BROADBAND OPTICAL FIELDS WITH APPLICATIONS TO WHITE-LIGHT SHEARING INTERFEROMETRY		5. TYPE OF REPORT & PERIOD COVERED MS THESIS 6. PERFORMING ORG. REPORT NUMBER
7. AUTHOR(s) Paul S. Idell, 2nd Lt, USAF		8. CONTRACT OR GRANT NUMBER(s)
9. PERFORMING ORGANIZATION NAME AND ADDRESS Air Force Institute of Technology (AFIT/EN) Wright-Patterson AFB OH 45433		10. PROGRAM ELEMENT, PROJECT, TASK AREA & WORK UNIT NUMBERS
11. CONTROLLING OFFICE NAME AND ADDRESS Electro-Optics Section (OCSE), Strategic Surveillance Division, Rome Air Development Center, Griffiss AFB NY 13441		12. REPORT DATE December 1978 13. NUMBER OF PAGES 109
14. MONITORING AGENCY NAME & ADDRESS (if different from Controlling Office)		15. SECURITY CLASS. (of this report) UNCLASSIFIED 15a. DECLASSIFICATION/DOWNGRADING SCHEDULE

16. DISTRIBUTION STATEMENT (of this Report)

Approved for public release; distribution unlimited.

17. DISTRIBUTION STATEMENT (of the abstract entered in Block 20, if different from Report)

18. SUPPLEMENTARY NOTES

Approved for public release; IAW AFIT 190-17

1-23-79

JOSEPH P. HIPPS, Major, USAF
Director of Information

19. KEY WORDS (Continue on reverse side if necessary and identify by block number)

Coherence	Shearing Interferometer
Optics	Interference
Broadband Light	Atmospheric Turbulence
White-Light	Phase Compensation
	Compensated Imaging

20. ABSTRACT (Continue on reverse side if necessary and identify by block number)

A free-space propagation model for broadband optical fields is developed based on a Karhunen-Loeve (KL) expansion of the time-varying portion of a coherence separable broadband optical envelope. The resulting modal expansion provides an intuitively simple interpretation of the propagation of broadband fields, and allows the output field correlation to be easily calculated. The propagation model is applied to the analysis of a lateral shear AC interferometer, which has been used to measure the spatial phase variations of a white-light

DD FORM 1 JAN 73 1473 EDITION OF 1 NOV 65 IS OBSOLETE UNCLASSIFIED

Cover Page

SECURITY CLASSIFICATION OF THIS PAGE (When Data Entered)

optical field envelope located at its input aperture. It is found that the interferometer's operation for broadband fields causes the phase which is measured by the interferometer to be related to a spatially filtered version of the aperture field. The propagation model is applied to the shearing interferometer's operation as a wavefront sensor in a phase-compensated imaging system, where the phase of the aperture field envelope has been disrupted by atmospheric turbulence. The turbulence-induced phase perturbation is modeled as a unit-modulus phase screen introduced at the aperture plane of the interferometer for each temporal mode of the field expansion.